POLITECNICO DI TORINO

Degree course in Mechatronics Engineering

Master of Science Thesis

Lateral dynamic control of vehicle steering position in low speed characteristics

Supervisors: **Candidate:**

Prof. Massimo Violante   Farangis Keyvani

December 2018

Abstract

These days autonomous driving systems are being widely researched and developed by automotive industries which has many subcategories related to different part of the vehicle. Each part singly acts the important role to have a safe and relaxed trip for human kind. This thesis is assigned to analyze the steering part of the vehicle which has the key role in the whole vehicle steerage.

The thesis intention is analysing friction factor in driver assistant system model in auto vehicles in controling the steering angle position in low speed driving and prepare a realistic model to test a new actuator system connected to the steering column.

This work is emphasizing on modeling the Steering column part of the vehicle particularly considering the linear friction of the rack and pinion. Also, three strategies of controller designed through MATLAB simulink to find the best results to control the steering angle position in a real-time simulation specially with respect to the linear friction of steering part and nonlinear friction of the road and tire which is prepared by IPG CarMaker software.

The steering column part can be modeled based on Lagrange and bong graph approaches and implemented through matlab simulink block diagrams verified by real vehicle data provided by Fiat CRF.

The control strategies which are commonly used in automotive industry are exploited as PID and MPC controller. PID auto tunning block diagram , PID with derivative in feedback loop and the MPC block simulation are required to track the input motor torque trough the output of the EPS model to control the steering angle position with respect to the frictions.

To implement the designed model of the EPS compound with the controller in the real-time simulation of IPG Carmaker, the best and tunnable controller is chosen to add inside the generic

CarMaker model through the vehicle control block which should be working in the specified maneuver of defined speed with sinusoidal, sinus sweep and IPG driver inputs tracking the output steering angle position.

Dedication

I dedicate this work to my parents, Ardeshir and Mahvash whom spent all their attempts and knowledges to be the best reliance in all dimensions of my life if I fail or rise. Special thanks to my dearest sister, Doctor Mahsa, with her endless supports who advise me excellence in professional and emotional life and thanks a billion to the kindest sister, Mahboobeh, who is one of the successful person I have seen and teach me how time and patience can arise human to be the best. I am so happy to have best family and friends whom have their footprint all over each step of my success.

Acknowledgment

Table of content

Table of figure

1.Introduction

Nowadays, automotive industry attempt to develop its technologies by using more electronic control and embedded software-based units which is more precise and rapidly replacing mechanical and hydraulic systems. This development, also has economic reasons in case of hardware component cost, performance and reliability. Also, provides testability in early phase of designing in all vehicle fields.

1-1 Automotive project cycle

Generally, in automotive industry to represent the system development life cycle more precisely, a famous graphical model is used to summarize the main steps to be taken for developing the testing model. This graphical model is called V-cycle.
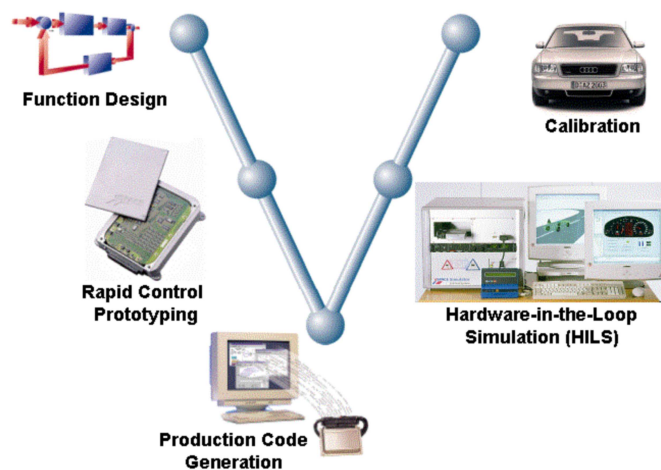
Figure 1. Automotive V-cycle

The V-cycle is stablished where, real time system performance and high speed feedback control is required. The V-cycle controller is applied to software development of automobile ECU by manufacturers and suppliers. Its configuration process can be done by model constructed by a simulation software which should be a standard tool in control area to handle non-linear systems. Then, the model should be validated in a real-time operation with actual plant. As the next step, the controller validated model should be manually programmed to be implemented on target hardware. Hardware in loop simulation also is used as an alternative actual plant testing to decrease the test cost and reduce the risk of accidents due to the software bugs. The final process of the V-cycle is for tuning the controller parameters to get the acceptable results for the users.

In the design flow of the model, V-cycle can be represented. Which contains different steps as requirement analysis, functional specification to analyze a problem and possible solution, high level design to design a possible solution by software architecture, detailed design or program specifications which includes Simulink and model in loop testing, embedded coder to approach the software behavior, unit testing to validate the used software, integration testing that deploy the software on an embedded computer which is hardware in loop testing, system testing and user acceptance testing. Fig.2. shows the general design point of view.
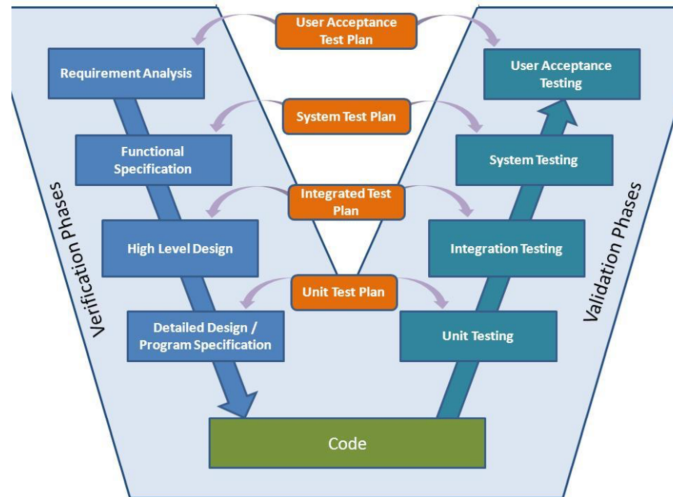
Figure 2. general V-cycle

Here, the thesis is limited mostly to the verification phases and going to be ready for the next phases test in Fiat CRF test benches.

1-2 steering part of the vehicle

As the steering system is a main part of the vehicle in receiving the driver tasks control, it is so effective to equipped mechanical handling steering system with power assistant components.

Electrically controlled or powered of steering system can be in three different ways that developed one by one, Hydraulic (HPS), Electro-Hydraulic (EHPS) and Electric (EPS) that they are safe, energy saver, less area overhead and independently engine supplying. The most frequent and newest one is EPS.

EPS system is typically considered as electric servomechanism which is including four general parts of steering column, controller, electric motor and sensor.

In EPS, there is an electric motor in steering column or steering gear to apply the torque to steering wheel which divided in two classes of brushless DC motor by square wave input and permanent magnet synchronous motor by sinusoidal input waveform. Then, there is a sensor for detecting the steering wheel position. Also, a control module used to provide input voltage for servomotor called ECU which can be a developed PID or MPC controller to increase stability. And the last part will be steering mechanism that receive the driver's torque and electric motor assistant torque then, provide steering and gear angle for sensor.

Steering wheel angle position control refers to steering driver's signal which in kinematic form is steering wheel angle and in dynamic form is steering wheel input torque. And, power assistant signal that its powering is on steering shaft or is bellow steering gear so, we have steering gear assistant torque. In addition, sum of the aligning and distractive signals cause external torque for right and left wheels. The output signal is provided for vehicle motion that is steered wheel angle.

1-3 Software

In order to model the steering column part of the vehicle and have a rigorous controller, the best and reliable area could be MATLAB Simulink which can be connected and work synchronously with another software which is called IPG Carmaker. This software, is well known among the automotive companies which can provide the virtual test driving and has the real-time model of the produced vehicle specially in Germany.

1-4 Objective

The main goal of this thesis is developing a new model for vehicle steering position control at low speed in case of parking situations. The model should consider the characteristics which are specially affected at low speed and high steering angle. Also, the friction and non-linear forces from the wheel part are became important.

2. Literature review

There are a lot of papers and thesis available on the EPS topic and related control fields. Oh and Chae (2004) did their research on the steer by wire system modeling and control algorithm based on bond graph approaches. Many papers on EPS topics have been published so far. Chen and Chen (2006) used Newton's law to build the dynamic model while Parmar and Hung (2004) utilized the Lagrange's equations to construct the dynamic equation of the EPS system. The authors present a strategy that eliminates the steering column torque sensor, a critical component in existing EPS controller designs. Liao and Du (2003) combined Matlab/Simulink and Adams to simulate the behavior of the EPS system on the vehicle motion. Choi et al. (2007) associated Sim Power System with Matlab/Simulink to describe the effect of power electronics on the EPS system, meanwhile, Kurishige and Kifuku (2001) introduced a new EPS control system that reduces steering torque during static steering. The stability of the EPS system is analyzed by Li and Wenjiang (2008) based on the mathematics model for pinion and rack steering system. A fuzzy control method for actively reducing pressure ripples for EPS system is proposed by Li et al. (2009). Within the two papers published, Chabaan (2009a, b) described an optimal control method, H infinity, for improved performance and robustness of electrical steering systems. A new linear quadratic regulator (LQR) controller proposed by Wenchang and Hongqi (2011) uses the steering wheel angle, yaw rate, and the sideslip angle as the optimization object. In Chalmers university Bhat and Malghan (2016) try to model the steering system and analyze the vehicle performance in the virtual vehicle environment which serves as a platform to perform vehicle level verification for modeling and simulation of physical plant model and controller in IPG Carmaker.

Throughout the history, steering system provide the interaction between the driver and wheels. Different systems can be used to achieve this interaction while in the early stage of car history, because of the difficulties in steering of two front wheels, a three-wheeled car was developed by Carl Benz and Gottlieb Daimler in 1886 but it did not take too long to introduce two-wheel steering system in 1893 and used it in the mass-produced car called Benz Velo.
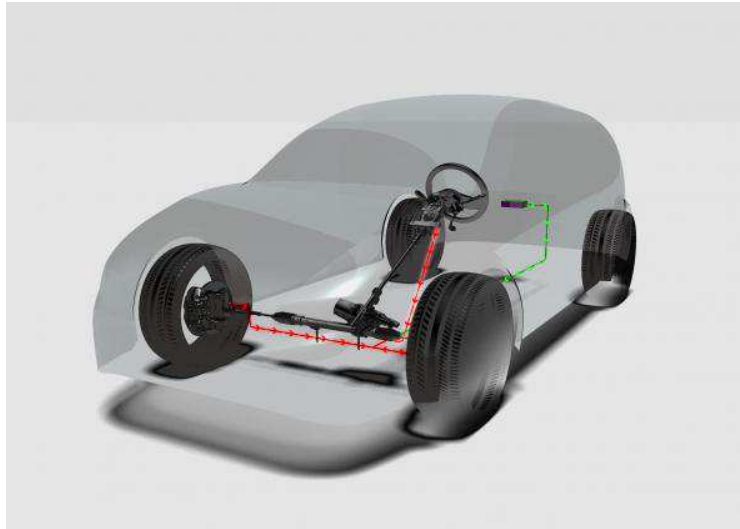
Figure 3. general view of steering system

Many different system have been introduced but a simple and most common one is rack-and-pinion steering which contains a pinion gear compound with a gear rack to convert the rotational movement of steering wheel to the translation movement of the steering rack.

Figure 4 rack-and-pinion

To move the steering rack a large torque from steering wheel is needed so, in the past, to compensate this torque, large steering wheels were provided this leverage. But now power assisted steering is to provide an assisting torque on the input shaft or an assistant force on steering rack. There are different power assists available which the most usable ones are the hydraulic systems, the electro-hydraulic systems and electric power assistant systems(EPAS).

In any way, steering system is substantial part of the vehicle to operate. For assisting the driver to turn the steering wheel in the situation of fully effort turning like in parking area or when the vehicle weight increased, Power steering system is introduced.

Power steering helps the driver of a vehicle to steer by directing some of its power to assist in swiveling the steered road wheels about their steering axes. As vehicles have become heavier and switched to front wheel drive, particularly using negative offset geometry, along with increases in tire width and diameter, the effort needed to turn the wheels about their steering axis has increased, often to the point where major physical exertion would be needed were it not for power assistance. To alleviate this auto makers have developed power steering systems, or more correctly power-assisted steering, since on road-going vehicles there must be a mechanical linkage as a fail-safe.

There are two types of power steering systems: hydraulic and electric/electronic. A hydraulic-electric hybrid system is also possible.

2-1 Hydraulic power steering

A hydraulic power steering (HPS) uses hydraulic pressure supplied by an engine-driven pump to assist the motion of turning the steering wheel. This system works thanks to a liquid under pressure which, controlled by an appropriate valve assists the steering of the driver. Thus, the main components of the hydraulic guide are: a tank for the liquid, liquid conduction pipes, a pump that carries the liquid under pressure, a valve that allows the liquid to act during the steering and a seat that guarantees the sealing of the liquid.

The pump that carries the pressurized liquid is driven by the crankshaft and rotates continuously When the steering is turned, the rotary motion is transmitted to the input shaft and from this to the valve, which must guarantee the flow of the liquid in the right quantity according to various parameters such as steering torque, angle and speed. This flow is sent into the piston unit obviously in a direction that is in line with the direction of the steering. The piston is fixed to the pinion which, meshes with the teeth of the crepe, transforming the rotary motion into rectilinear motion. Important requirement is the hydraulic seal of the seat in which the rack runs. in fact, the latter is in effect a piston, pushed by the liquid under pressure and if losses occur, the whole system is compromised.

This system although it offers the assistance in driving and operational safety, also has some disadvantages such as size and presence of polluting liquids. moreover, there is a high consumption

since the pump being directly connected to the vehicle's engine, is always in operation even in times of running in a straight line. The system described above is shown in figure 5.
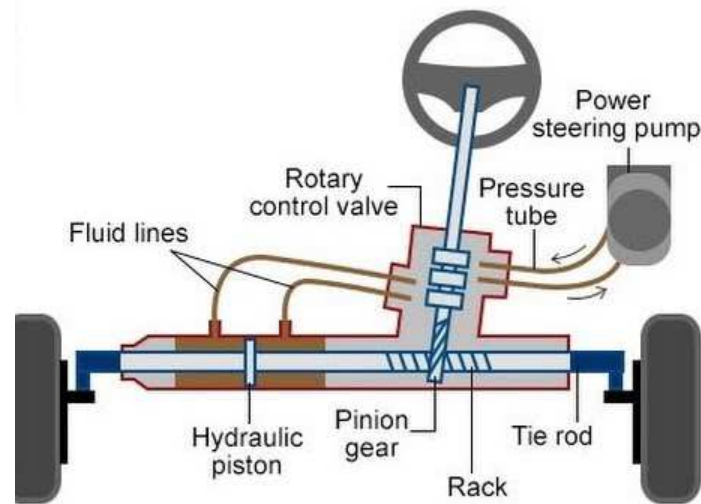
Figure 5. hydraulic power steering system

Mostly, power steering systems are hydraulic while the electric one has the advantages of energy saving, stability and safety, environmental protection and less weight in comparison with hydraulic one due to loss of hydraulic pump and fluid, hoses, drive belt and pulley on the engine. In addition, for the passenger cars, active damping and return, angle detection logic and friction compensation are somehow benefits for the driver.

The EPS system can be considered a conventional steering system based on a pinion / rack to which a system that generates the assisted torque with an electric motor is added, as well as required for an assisted steering. When the driver makes a steering and then applies a torque on the steering, the system detects the intensity of the force exerted and based on which it drives by means of an appropriate current, the electric motor which is put in rotation. Then, obtaining a further torque on the steering column and reducing overall the effort necessary for the driver to perform the desired maneuver.

Electric power steering (EPS) is more efficient than hydraulic power steering, since the electric power steering motor only needs to provide assistances when the steering wheel is turned, whereas the hydraulic pump must run constantly. In EPS, the amount of assistance is easily tunable to the vehicle type, road speed, and even driver preference. An added benefit is the elimination of environmental hazard posed by leakage and disposal of hydraulic power steering fluid. In addition, electrical assistance is not lost when the engine fails or stalls, whereas hydraulic assistance stops working if the engine stops, making the steering doubly heavy as the driver must now turn not only the very heavy steering but also the power-assistance system itself.

2-2 Steer-by-wire

On the other hand, there is another kind of system which provide steering control with fewer mechanical components and linkages between the steering wheel and the front wheels. System is controlled by an ECU through electric wires. The SBW system is divided in two parts of a steering wheel and front wheels and based on two electronic actuators assisting in their operation. These two actuators receiving input signal from the ECU, then one actuator generate reactive torque to the steering wheel while the other one steers the front wheel according to the driver's command.
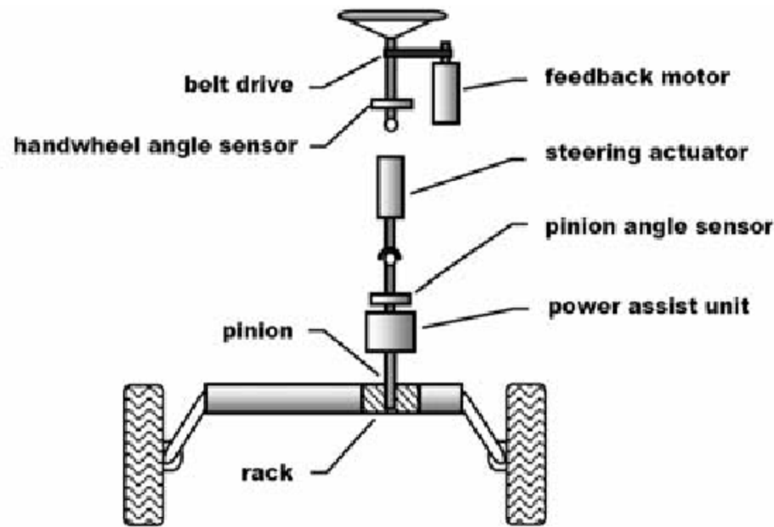
Figure 6. steer-by-wire system

More precisely, Steer-by-Wire technology generally, is based on mechanical components, microcontrollers, real-time software, actuators, power electronics and digital sensors. angular and torque sensors; for the steering wheel and the front wheels. Actuators; for force feedback on the steering wheel and for the movement of the wheels. power electronics; to drive the actuators. Microcontrollers; to ensure correct steering angle and feedback force, mechanical components; such as steering, gearbox, torsion bar, pinion, rack and wheels.

The elimination of the mechanical connection creates two interconnected subsystems only from the electronics hand-wheel and road-wheel; the first is represented by the steering unit. the second by the rack-pinion system and front wheels. For each subsystem, there is the presence of an actuator; the steering actuator, which generates a feedback force on the steering wheel and the front wheel actuator, which controls the latter.

There are two different control problems for a Steer-by-Wire system:

On the one hand, it is necessary to ensure that the steering angle determined by the guide is accurately followed. therefore, the input of the control torque provided by the driving motor must ensure that the angular position of the directional control system follows the input imposed by the guide. On the other hand, it is essential to provide the driver with a realistic "virtual driving perception". For this purpose, a reference pair must first be generated. the driving torque provided by the steering motor must then ensure that the resistive torque felt on the steering wheel follows the reference torque.

Steer by wire system can be considered as a stage of evolution from mechanical steering to steer by wire system, but its disadvantage can be hacking problem which cause faulted control or shut off by either wired or wire-less connection. The first production vehicle to implement this was the Infiniti Q50. but after negative comments they retrofitted the traditional hydraulic steering. Its implementation in road vehicles is limited by concerns over reliability although it has been demonstrated in several concept vehicles such as ThyssenKrupp Presta Steering's Mercedes-Benz Unimog, General Motors'Hy-wire and Sequel, Saabs Prometheus and the Mazda Ryuga. A rear wheel SBW system by Delphi called Quadrasteer is used on some pickup trucks but has had limited commercial success.

2-3 Electric Power Steering architecture

Electric Power Steering is an alternative for the traditional mechanical and hydraulic steering motor which is using an electric motor to assist steering the vehicle when the steering wheel is turned.

Design strategies for keeping the original steering wheel systems, use a gear to select between manual and autonomous steering control position. To fed this gear, power supply received by vehicle's battery is needed which leads to automatically moves the steering wheel by selecting a Dc motor attached to the two gears. So, motor power become critical because it is fed from vehicle battery therefor, more power and charge is needed which can be compensate by increasing the maximum current. This Dc motor can be controlled through a PID controller. In manual steering control, based on the time needed to turn the steering wheel by driver and calculation of turning speed goes to the input of the controller. As the purpose of this thesis, the automatic steering control data is more important which needs the motor torque to turn the steering wheel and provide the required input for ECU. The controller needs a power voltage more than the voltage provided by DC motor so, the power supply comes from a DC-DC converter. In case of stopped vehicle, higher torque is needed for starting point. Besides, to determine the initial position of steering wheel, a homing sensor is used. Instead of DC motor, there is another option with the same capacity ordinary motor but smaller and lighter with lower rotor rotary inertia which is more suitable for high torque responses that is permanent magnet synchronous motor (PMSM). There are different structures available for PMSM, the easy to control one is considered for EPS as surface convex PMSM which assume that motor iron core saturation and leakage flux are ignored and exclusive eddy current and hysteresis losses can be neglected and it uses three-phase sinusoidal current in motor.

Failure and mistakes happened in EPS systems could be because of loss of torque control due to short or open circuit in motor coil or damaged motor driver which leads to lack of motor inertia to assist the driver or unintended motor torque which cause unwanted steering without input from the

driver or assistant motor. These two failure should be considered during the hardware-in-loop test while in the design point of view in this thesis the role of linear and nonlinear friction caused in the steering column and in the vehicle tire and road area might be so critical to consider in design calculations.

To properly capture the response of the steering system a sophisticated model is required. The model should include the frictions, gear ratios, inertias and compliances from the steering wheel down to the tie rods. The steering system modeling refers to a spatial multi-body on the car-body system. Spatial movements of the steering wheel change the wheels' motions geometry that can be characterized by kinematic equations and dynamic model that can be supplemented by electric and mechatronic components like motor, sensor and regulator which have small moment of inertia and suitable for autonomic subsystems.
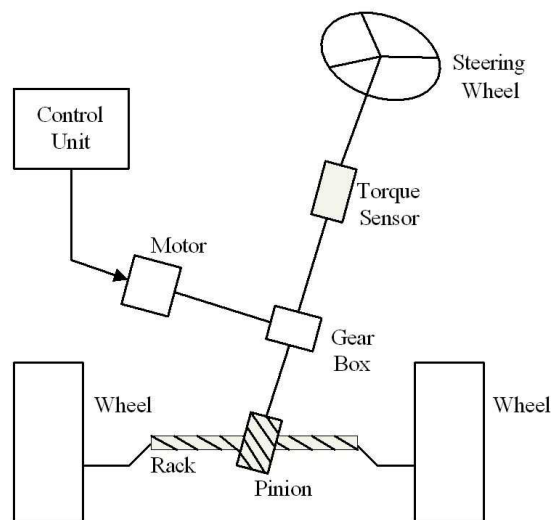
Figure 7. EPS architecture

To provide assist to the driver torque sensor is needed, which measures the driver's torque and sends a signal to the controller proportional to this torque. The controller also receives steering

position information from the position sensor that is collocated with the torque sensor and together they make up the Sensor. The torque and position information is processed in the controller and an assist command is generated. This assist command is modulated by the vehicle speed signal, which is also received by the controller. This command is given to the motor, which provides the torque to the assist mechanism. The gear mechanism amplifies this torque, and ultimately the loop is closed by applying the assist torque to the steering column. The schematic view of the steering column available in figure 7.

Other EPS architectures such as Rack Assist and Pinion Assist. have been proposed by Delphi and others. These different configurations, while important with respect to packaging or environmental effects that is not so relevant to this thesis subject.

In this case, the rack and pinion model is not considered. And a simple Dc motor is sufficient without any motor dynamics, low level control and motor characteristics.

2-4 Disturbance and Friction

Furthermore, Friction plays an important role in the dynamic behavior of the system. The two considerable frictions in this thesis will be the self-aligning torque at the front wheel which is more dependent to the vehicle velocity. And the other one is non-linear tire stiffness.
For linear control approach the steering system must be linearized. Therefore, friction is modeled as a viscos damping, constant gear ratios and linear vehicle model are used.

2-4-1 self-aligning torque:

The external forces acting on the steering rack come from the lateral and longitudinal tire forces and are transmitted through the upright and steering arm to the tie rods. When the vehicle is in motion and the wheel angles are larger than zero, the lateral forces act to bring the wheels and steering wheel to their original position. The reason for this is that a pneumatic tire has asymmetric deformations around the contact patch leading to an uneven distribution of the lateral forces.
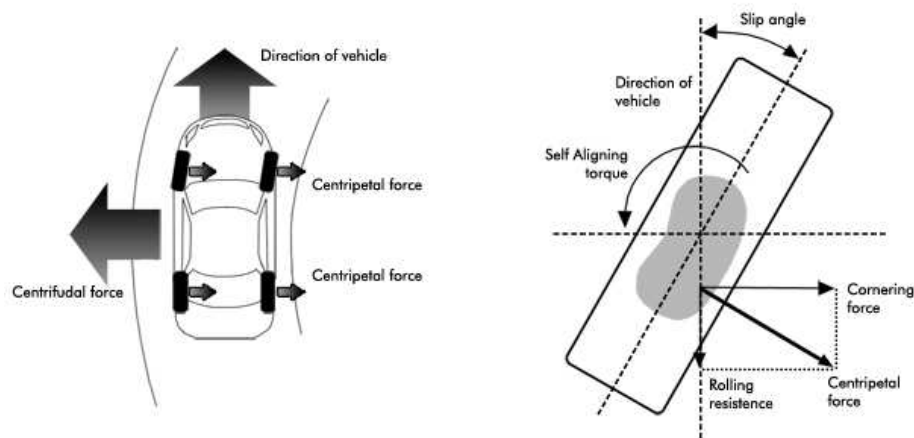
Figure 8. self-aligning torque schematic

2-5 controllers

Control systems are used to manage components which are needed for a condition or an output to obtain. The word 'control' itself shows the command over any system. It is controlled when the systems are stable.

An open-loop control system takes input under the consideration and doesn't react on the feedback to obtain the output. There are no disturbances or variations in this system and works on fix

conditions. So, this method can be useful to test the model in ideal condition without any disturbance and compare it with the situation of different disturbance excitation. the closed-loop system also referred to a feedback control system which records the difference between the actual output and the desired one instead of input. The major issue of a closed-loop system is stability and make the non-linear changes on system gain.

In this thesis, the frictions and disturbances are important to consider so the control strategies are mostly based on closed-loop systems.

2-5-1 PID

PID (proportional integral derivative) control is one of the earlier control strategies. Its early implementation was in pneumatic devices, followed by vacuum and solid state analog electronics, before arriving at today's digital implementation of microprocessors. It has a simple control structure which was understood by plant operators and which they found relatively easy to tune. Since many control systems using PID control have proved satisfactory, it still has a wide range of applications in industrial control. According to a survey for process control systems conducted in 1989, more than 90 of the control loops were of the PID type. PID control has been an active research topic for many years. Since many process plants controlled by PID controllers have similar dynamics it has been found possible to set satisfactory controller parameters from less plant information than a complete mathematical model. These techniques came about because of the desire to adjust controller parameters in situ with a minimum of effort, and also because of the possible difficulty and poor cost benefit of obtaining mathematical models. The two most popular PID techniques were the step reaction curve experiment, and a closed-loop "cycling" experiment

under proportional control around the nominal operating point.

In this thesis, two model of useful PID-type controller design techniques going to be presented, and implementation issue for the algorithms also be discussed.

2-5-2 MPC

Model predictive control (MPC) is an advanced method of process control that is used to control a system while satisfying a set of constraints. It has been in use in the industries like chemical plant and oil refineries since the 1980s. In recent years, it has also been used in power system balancing models and in power electronic. Current use of MPC are in most of existing multivariable control applications, Technology of choice for many new advanced multivariable control application, Success rides on the computing power increase and Has many important practical advantages.

Model predictive controllers rely on dynamic models of the process, most often linear empirical models obtained by system identification. The main advantage of MPC is the fact that it allows the current timeslot to be optimized, while keeping future timeslots in account. This is achieved by optimizing a finite time-horizon, but only implementing the current timeslot and then optimizing again, repeatedly. Also, MPC can anticipate future events and can take control actions accordingly. PID controllers do not have this predictive ability. MPC is nearly universally implemented as a digital control. The overall objectives of an MPC controller have been summarized by Qin and Badgwell (2003). Which are: 1-Prevent violations of input and output constraints. 2-Drive some output variables to their optimal set points while maintaining other

outputs within specified ranges. 3-Prevent excessive movement of the input variables. 4-Control as many process variables as possible when a sensor or actuator is not available.

he MPC calculations are based on current measurements and predictions of the future values of the outputs. The objective of the MPC control calculations is to determine a sequence of *control moves* so that the predicted response moves to the set point in an optimal manner. The actual output *y*, predicted output, and manipulated input *u* for SISO control. At the sampling instant, denoted by *k*, the MPC strategy calculates a set of *M* values of the input {*u(k+i-1)*, *i=1, 2, . . ., M*}. The set consists of the current input *u(k)* and *M-1* future inputs. The input is held constant after the *M* control moves. The inputs are calculated so that a set of *Ps* predicted outputs {*y(k+i)*, *i=1, 2, . . ., P*} reaches the set point in an optimal manner. The control calculations are based on optimizing an objective function. The number of predictions *P* is referred to as the *prediction horizon* while the number of control moves *M* is called the *control horizon*. The MPC predictions are made using a dynamic model, typically a linear empirical model such as a multivariable version of the step response or difference equation models. Alternatively, transfer function or state- space models can be employed. Step-response models offer the advantage that they can represent stable processes with unusual dynamic behavior that cannot be accurately described by simple transfer function models. Their main disadvantage is the large number of model parameters. Although step-response models are not suitable for unstable processes, they can be modified to represent integrating processes. Also, Similar predictions can be made using other types of linear models such as transfer function or state-space models. The step-response model of a stable, single-input, single-output process can be written as bellow:

$$y(k + 1) = y_0 + \sum_{i=1}^{N-1} S_i \Delta u(k - i + 1) + S_N u(k - N + 1) \tag{1}$$

where $y(k+1)$ is the output variable at the $(k+1)$ sampling instant, and $u(k-i+1)$ denotes the change in the manipulated input from one sampling instant to the next, $u(k-i+1) +u(k-i+1)-u(k-i)$. Both y and u are deviation variables. The model parameters are the N step-response coefficients, S_1 to S_N. Typically, N is selected so that $30 \leq N \leq 120$. The initial value, y (0), is denoted by y_0. For simplicity, $y_0=0$.

2-6 IPG CarMaker

IPG CarMaker is provided for real-time full vehicle simulation aimed for fast simulation which is using multibody simulations about kinematics and compliance, advanced tire models, aerodynamics and three dimensional dynamics calculations. This program has the benefit of being able to simulate faster than real time by utilizing lookup tables for kinematics and compliance in combination with a tire model of choice. Another benefit is that any system of the vehicle in CarMaker can be replaced with a custom one in a Simulink environment, which in this project would be a custom steering system model created by the steering supplier.

When CarMaker and the steering system are connected, simulations can be run. What needs to be defined to run these simulations are the maneuvers (with a set speed, steering wheel angle input, pre-defined lateral acceleration, road surface) and, if applicable, extra load. The maneuvers used in this research are Volvo Cars standardized test procedures for steering DNA testing (the same procedures used in physical tests).

In CarMaker, the vehicle model is divided into five parts; four wheel carriers with wheels which are connected (sprung masses) and vehicle chassis (unsprung mass). Each part has separated mass and inertia around each Cartesian axis (I_{xx}, I_{yy}, I_{zz}).

Three main coordinate systems exist, which are Fr1, Fr2 and the center of mass. Fr1 is the reference coordinate at the rear and center of the vehicle and Fr2 is each wheel individual coordinates. The forward direction of the vehicle always point the x-axis and the perpendicular direction could be the y-axis.
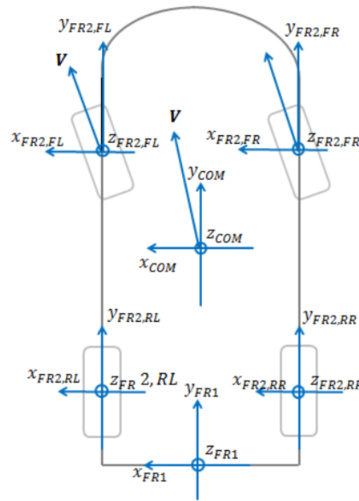

Figure 9. Coordinate system of CarMaker

Using objective metrics as a way of tuning and evaluating vehicle parameters and tires is commonly used due to its upside of creating reproducible results. It is also a way to compare and assess vehicles numerically which cause Accuracy, fast and less costly than conventional physical testing. steering wheel angle, steering wheel torque, lateral acceleration, yaw rate and roll velocity. CarMaker is a self-sufficient software that does not require any specific software environment to work, nevertheless, it can be coupled with Simulink to increase the control possibility.

3. EPS modeling and simulation

according to the thesis goal, to represent the EPS working mechanism in a schematic view as figure 10, there is a block of steering wheel equation which, contains steering dynamic equations and motor part equations. Also, there is a control block which has the input of the reference of the steering position in comparison with the feedback of the actual steering position. The controller output is going to be the motor torque which, is the input of the steering equation block in motor part. The motor angle position calculated in motor part will take in to account for the steering part along with the steering wheel torque which is coming from the driver. At the end, we will have controlled steering angle position which is tracking the input reference.
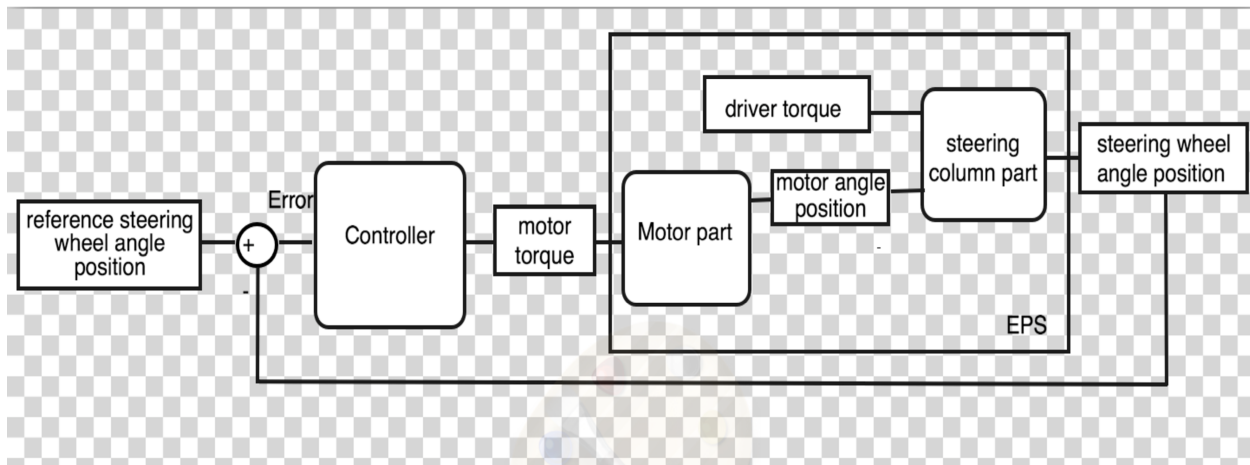

Figure 10. general EPS overview

The reference steering angle position is supplied from the CarMaker vehicle model.

3-1 steering column modeling

The steering system, from mechanical point of view perhaps is made of many masses and inertias connected with springs and dampers. while, this high stiffness cause higher frequency modes

which is usually inconsequential to the fundamental behavior of the system that is dominant by the lower frequency modes. So, simply reduction in modelling order stems can be allowed. The model reduction can be introduced by considering the rack and pinion and the tie rod connection which are going to enter the simulation through the carmaker vehicle model.

Specifically, the steering block is going to be analyzed and its dynamic model equations are going to be represented. EPS dynamic model is shown in figure 12 which is a sample of steering dynamic model with driver torque $T_d(N.m)$, steering position $\theta_s(rad)$, steering wheel inertia $J_s(Kg.m^2)$ and torsion bar stiffness $K_s(N.m/rad)$, steering wheel viscous damping $B_s(N.m.s)$, motor viscous damping $B_m(N.m.s)$, rotary inertia of assistant motor $J_m(Kg.m^2)$, and motor position θ_m (rad).

Generally, system representing the driver input being transmitted from the steering wheel to the rack via the steering column, torsion bar and pinion gear and the second part being the servo motor input through the output shaft to the rack via the belt and the ball nut-gear. The mechanical system was modelled by using the setup in Figure 12 including the combined inertia of the steering wheel and steering column, the compliance of the torsion bar, hardy disc and column as well as the inertia of the steering rack.
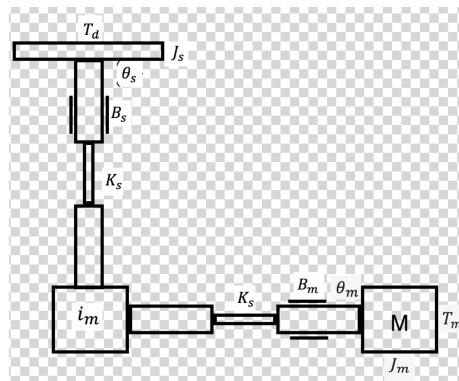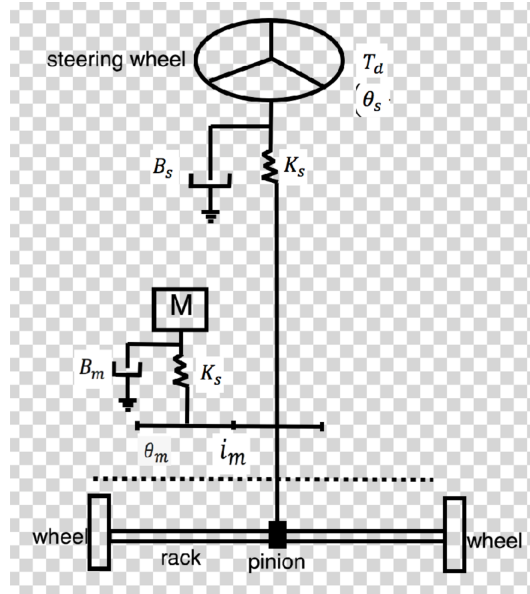

Figure 11. EPS dynamic model

Figure 12. EPS schematic structure

The mechanical steering system components of EPS can be described as steering wheel by the inertial components and steering column and shafts to represent rotational axis of the model, damping and capacitive components which are steering axis moment of inertia.

To reach the steering position control modeling, first, it is important to find the mathematical model. In this way two approaches can be used. one of the basic way is using Lagrange equation which is based on the definition of total energy of the system and the other one is Bond Graph that is according to the power of the system.

3-1-1 Lagrange and Bond graph approaches

The formulation of the dynamic equations of a system, according to the Lagrange approach, is based on the definition of the kinetic co-energies and of the total potential energies of the system

itself. This approach allows to write many differential equations of the second order as there are N generalized coordinates.

The Lagrange function defines the difference between the kinetic co-energy C * and the potential energy P:

$$\mathcal{L}(q, \dot{q}) = \mathcal{C}^*(q, \dot{q}) - \mathcal{P}(q) \tag{2}$$

Where, the $\mathcal{C}^*(q, \dot{q})$ is total kinetic co-energy which is the function of generalized coordinates and velocity and $\mathcal{P}(q)$ is total potential energy as a function of generalized coordinates.

For each coordinate, q_i with $i = 1, ..., N$:

$$\frac{d}{dt}\left(\frac{\partial \mathcal{L}}{\partial \dot{q}_i}\right) - \frac{\partial \mathcal{L}}{\partial q_i} + \frac{\partial \mathcal{D}_i}{\partial \dot{q}_i} = \mathcal{F}_i \tag{3}$$

The term $\mathcal{D}_i$ represents the dissipation function of Rayleigh, linked to the forces due to friction phenomena, while the term $\mathcal{F}_i$ represents the i-th generalized force, with a positive sign if applied from the external environment to the body, with a negative sign if the other way around.

The Lagrange equations can be applied to different systems: mechanics, composed of individual rigid bodies; electromagnetic, identified by a circuit structure that connects components of an electric or magnetic type; electro-mechanics consisting of both mechanical parts and electromagnetic circuits We can define some similarities between the electrical quantities and the mechanical quantities, with regarding to the single terms of the equation 2; these analogies are shown in the following table:

	q	$\dot{q}$	$\mathcal{C}$	$\mathcal{P}$	$\mathcal{D}$	$\mathcal{F}$
Translation	x	$\dot{x}$	$\frac{1}{2}m\dot{x}^2$	$\frac{1}{2}\mathcal{K}_l\Delta\dot{x}^2$	$\frac{1}{2}\beta_l\dot{x}^2$	f
Rotation	θ	$\dot{\theta}$	$\frac{1}{2}\Gamma\dot{\theta}^2$	$\frac{1}{2}\mathcal{K}_a\Delta\dot{\theta}^2$	$\frac{1}{2}\beta_a\dot{\theta}^2$	τ
Effort	q	i	$\frac{1}{2}Li^2$	$\frac{1}{2\mathcal{C}}q^2$	$\frac{1}{2}R\dot{q}^2$	E
Flow	λ	e	$\frac{1}{2}\mathcal{C}e^2$	$\frac{1}{2L}\lambda^2$	$\frac{1}{2R}\dot{\lambda}^2$	I

Table 1. Lagrange electro mechanic analogies

The Bond graph theory is based on the concept of power exchanging between subsystems through ports interfaces and operate in all physics domain. The power P(t) is expressed as the product of intensity or effort derived with respect to the time p(t) of the moment generalized and variable flow derived with respect to the time of shift generalized q(t).

$$P(t) = e(t).f(t) = \frac{dp}{dt}.\frac{dq}{dt} \tag{4}$$

model construction of the Bond graph consists on connection between the two subsystem ports. to show the positive flow direction of power at a moment of time, subsystems are joined by half arrow and the variable intensity direction can be indicated by vertical section of causality or causal stroke which place at the end of the bond graph. The elements for interconnections are junctions which represents a generalization of Kirchhoff's laws in electrical networks. The flow junctions are showed with 1 and effort junctions showed by 0.

The elements which are used in this construction of steering column described as bellow:

- ○ Element R is the element of energy dissipation correspond to a damper so its relation is $e = \Phi R(f)$.

- ○ Element C is an accumulator of potential energy equivalent to stiffness so it is worth $q = \Phi C(e)$.

- ○ Element I is an accumulator of kinematic energy equivalent to inertia which has $p = \Phi I(f)$.

- ○ Element S_e is intensity generator.

- ○ Element S_f is flow generator.

- ○ Element TF is transformer which transforms intensity into intensity and flow in to flow.

- ○ Element GY is rotator which transform intensity into flow and vice versa which can be represented as motor part.

Now, by considering both Lagrange and Bond graph approaches and the EPS scheme, the EPS branch can be mathematically modelled.

$$q(t) = \begin{bmatrix} \theta_s \\ \theta_m \end{bmatrix} \tag{5}$$

$$C^*(q, \dot{q}) = \sum_i C_i(q, \dot{q}) = \frac{1}{2} J_s \dot{\theta}_s{}^2 + \frac{1}{2} J_m \dot{\theta}_m{}^2 + \frac{1}{2} J_r \frac{\dot{\theta}_m{}^2}{i_m{}^2} + \frac{1}{2} J_v \dot{\theta}_m{}^2 \tag{6}$$

$$P(q) = \sum_i P_i(q) = \frac{1}{2} k_s (\theta_s - \frac{\theta_m}{i_m})^2 \tag{7}$$

$$D(\dot{q}) = \sum_i D_i(\dot{q}) = \frac{1}{2} B_s \dot{\theta}_s{}^2 + \frac{1}{2} B_m \dot{\theta}_m{}^2 \tag{8}$$

$$F = \sum_i F_i = T_d + T_m \tag{9}$$

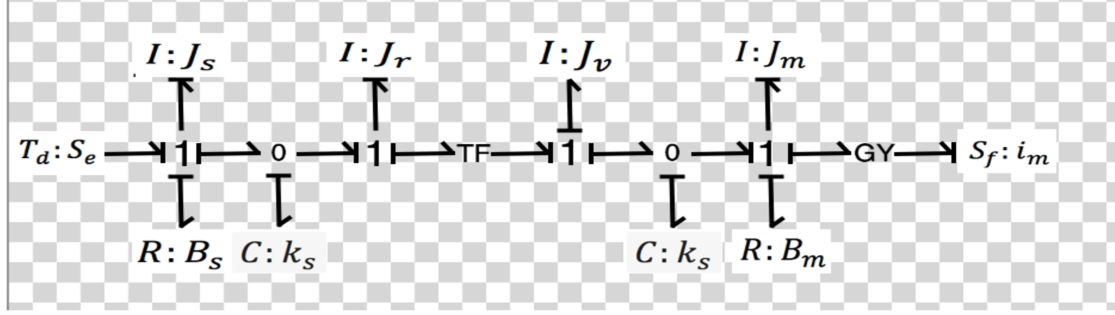So, from the equations the Bond graph is going to be like bellow:

Figure 13. EPS subsystem Bond Graph model

So, the Newton-Euler equations in steering column and motor part are derived from figure 6 which are:

$$J_s * \ddot{\theta}_s = T_d - K_s \left(\theta_s - \frac{\theta_m}{i_m} \right) - B_s * \dot{\theta}_s \tag{10}$$

$$J_{eq} * \ddot{\theta}_m = T_m + \left[K_s \left(\theta_s - \frac{\theta_m}{i_m} \right) \right] * i_m - B_m * \dot{\theta}_m \tag{11}$$

$$J_{eq} = J_m + J_v + \left(\frac{J_r}{i_m{}^2} \right) \tag{12}$$

3-2 self-aligning torque

The influence of tire-road friction in dynamic model which capture the self-alignment torque is important to consider. To find this phenomenon the model required to measure the side slip angle and angular velocity. For writing the equilibrium equation of steering system, it is mandatory to consider the friction phenomena which has serious consequences on the final results. The steering system operation is characterized by the transition of quiescence and turn which cause variations in steering velocity and zero-speed condition. So, friction of steering elements is changed from static to dynamic. Here, to model the friction torque of the tire and its influences on the upper part

of steering system, carmaker software is used which prepare the real-time road-tire friction torque consequences.

The upper part linear friction which is formed by rack and pinion contact and steering wheel bearings rolling and completely depends on steering wheel velocity. To find its mathematical formula in rack and pinion Dahl friction model which indicate that bearing friction behaved similar as solid friction, can be used. Dahl modeled the stress-strain curve by a differential equation. This friction model is a generalization of Coulomb friction but it produces a smooth transition around zero velocity. The frictional hysteresis at pre-sliding is approximated by a generalized first order equation of the position depending only on the sign of the velocity. Dahl proposed the following equation:

$$\dot{F}_f(t) = \sigma.\left[1 - \frac{F_f(t)}{F_c}.sign\big(\dot{x}(t)\big)\right]^{\lambda}.sign\left(1 - \frac{F_f(t)}{F_c}.sign\big(\dot{x}(t)\big)\right).\big(\dot{x}(t)\big) \quad (13)$$

where, $F_f(t)$ and F_c are Dahl friction force and column friction force respectively. $\dot{x}(t)$ is velocity between surfaces and λ is shape parameter.

σ is stiffness coefficient for steering wheel as bellow:

$$\sigma = \frac{2.B_S.K_S}{\sqrt{\frac{K_S}{Js}}} \quad (14)$$

$$\dot{T}_f = \sigma.sign(1 - \frac{T_f}{T_c}.sign(\dot{\theta}_s)).\dot{\theta}_s \quad (15)$$

where T_f and T_c are steering wheel friction torque and column friction level respectively.

Finally, to simplify this can be used in the main equations of the steering column:

$$T_f = \sigma.\theta_s \quad (16)$$

This linear friction torque is affected the torque produced by motor part of the vehicle. So, the final formula of the motor part to be obtained in (17) with considering the linear friction torque effect.

$$J_{eq} * \ddot{\theta}_m = T_m + \left[K_s \left(\theta_s - \frac{\theta_m}{i_m} \right) \right] * i_m - B_m * \dot{\theta}_m - T_f \tag{17}$$

Also, the state space equations can be written as bellow to simply model the formulas through MATLAB Simulink block diagram.

$$\begin{cases} \dot{X} = AX + BU \\ Y = CX + DU \end{cases} \tag{18}$$

$$\begin{bmatrix} \ddot{\theta}_s \\ \ddot{\theta}_m \\ \dot{\theta}_s \\ \dot{\theta}_m \end{bmatrix} = \begin{bmatrix} \dfrac{-B_s}{J_s} & 0 & \dfrac{-K_s}{J_s} - \sigma & \dfrac{-K_s}{i_m J_s} \\ 0 & -\dfrac{B_m}{J_{eq}} & \dfrac{K_s}{i_m J_{eq}} & \dfrac{-K_s}{i_m i_m J_s} \\ 1 & 0 & 0 & 0 \\ 0 & 1 & 0 & 0 \end{bmatrix} \begin{bmatrix} \dot{\theta}_s \\ \dot{\theta}_m \\ \theta_s \\ \theta_m \end{bmatrix} + \begin{bmatrix} \dfrac{1}{J_s} \\ \dfrac{1}{2J_{eq}} \\ 0 \\ 0 \end{bmatrix} T_m \tag{19}$$

$$\begin{bmatrix} \theta_s \\ \theta_m \end{bmatrix} = \begin{bmatrix} 0 & 0 & 1 & 0 \\ 0 & 0 & 0 & 1 \end{bmatrix} \begin{bmatrix} \dot{\theta}_s \\ \dot{\theta}_m \\ \theta_s \\ \theta_m \end{bmatrix} \tag{20}$$

which, produce the transfer function polynomial for steering position and motor position equation. To check the model validation, numeric values of parameters which are prepared by Fiat, to be considered. So, the Simulink model of the steering will be as figure 14 and The Bode graph of this transfer function can be represented as bellow in figure 16.
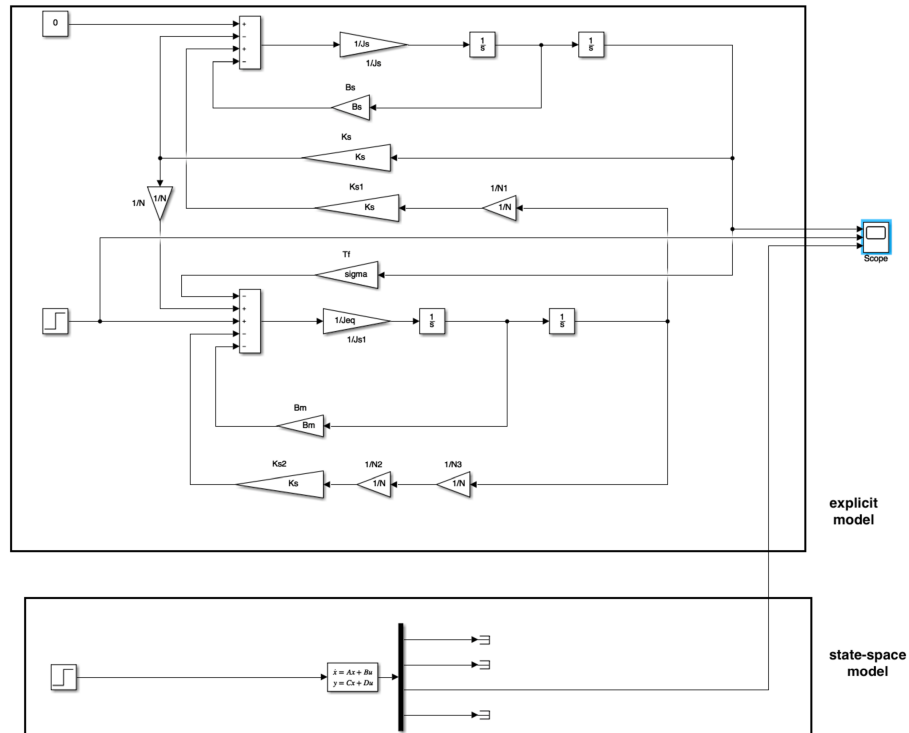
Figure 14. open-loop Simulink model of steering column with respect to the calculated equations considering the step input as the motor torque

The figure above shows the steering column Simulink model with respect to state space model and the explicit model. The transfer function is also used for defining the steady state block to check if the explicit model is working the same as the steady state model and designing the PID controller which has the reference and measured steering position as input to control.

For initial testing, it is enough to see primary acceptable result with zero driver torque and ideal step input response. The time responses of step input without any control strategy have big overshoot and resonance ripple as bellow in figure 15:
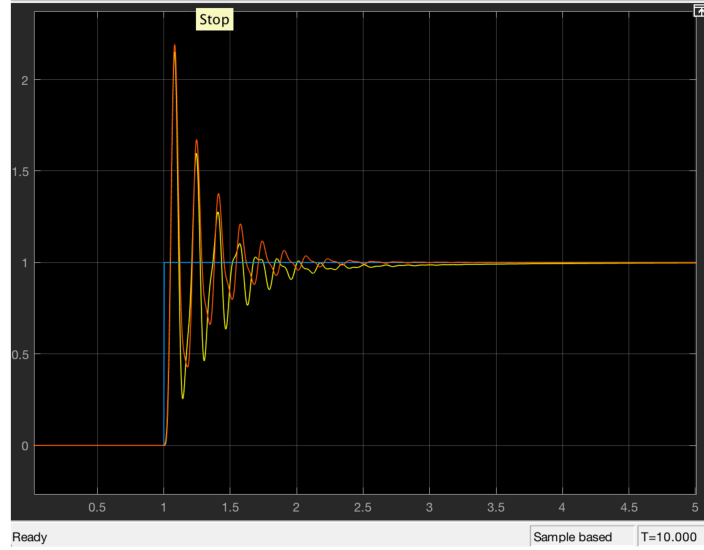
Figure 15. time response of steering column simulation without controller
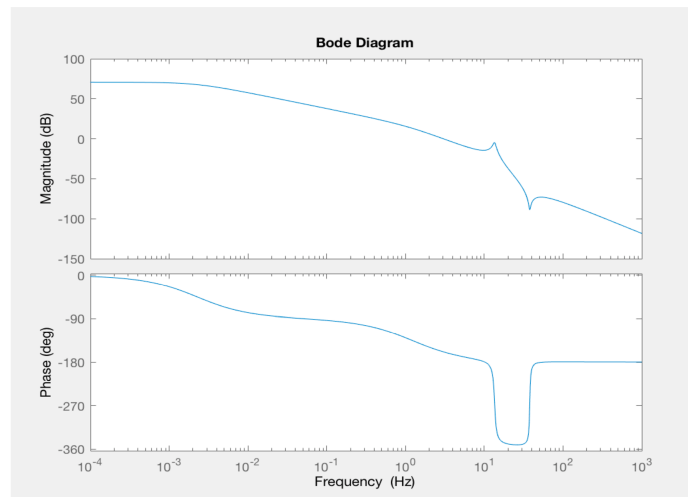
Figure 16. output transfer function of steering angle position with respect to motor torque

The frequency response shows that the steering wheel angle position start changing around 0.001Hz which is much lower than 1Hz which is expected.
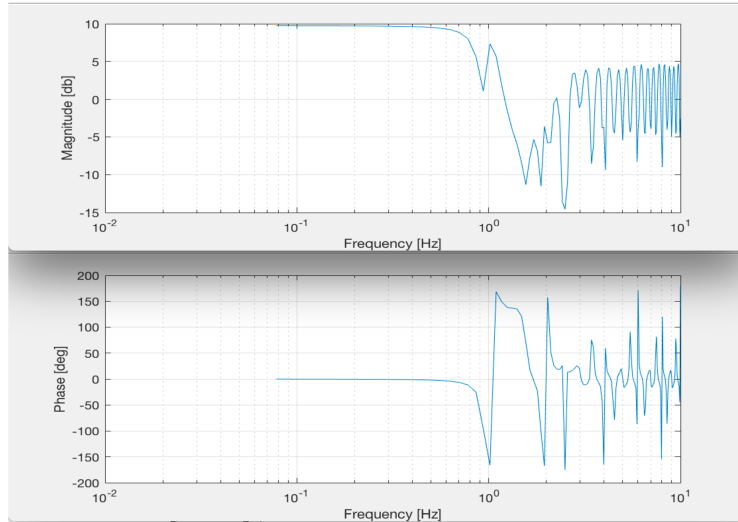
Figure 17. frequency response of EPS model with respect to step input as motor torque

Figure 17 shows that the bode diagram of the both transfer function and explicit model are nearly similar which are start to excite about 0.7 Hz before the noisy response of 1.7 Hz to the end.

For above diagram Transfer Function Estimate command is used. Transfer function estimator, estimate the system dynamic behavior from the simulation input and output signals which are both vectors of the same length then the bode diagram of the model can be concluded.

4. Controller actions

to test the controller actions a desired step input will be considered as a motor torque.

4-1 PID design and simulation

In PID controller design, different strategies can be used for tuning the PID coefficients which are numeric optimization algorithms and automatic tuning which is not allowing elegant analytic solution while, numerical methods are powerful practical techniques for controller design.

$$u(t) = K_p[e(t) + \frac{1}{T_i}\int_0^t e(\tau)d\tau + T_d\frac{de(t)}{dt}] \tag{21}$$

which it can be changed with respect to the system under control as bellow:

$$\theta_c(t) = K_p[\theta_e(t) + \frac{1}{T_i}\int_0^t \theta_e(\tau)d\tau + T_d\frac{d\theta_e(t)}{dt}] \tag{22}$$
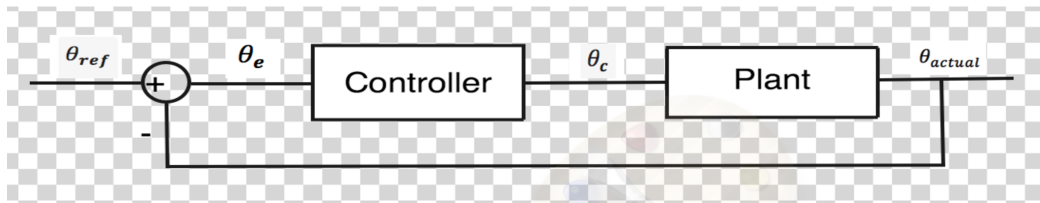
Figure 18. controller inputs and outputs

4-1-1 Auto-tuning PID

The first control strategy is using discrete PID block diagram and automatically tune it with the sampling time of 0.01 seconds. Which, has the tuned parameters as figure bellow:

Figure 19. tuned parameters of P, I and D in the Auto-tuning PID controller block diagram

The frequency response of the transfer function estimate and the time response of the Simulink

scope is available in figure 20 and 21.
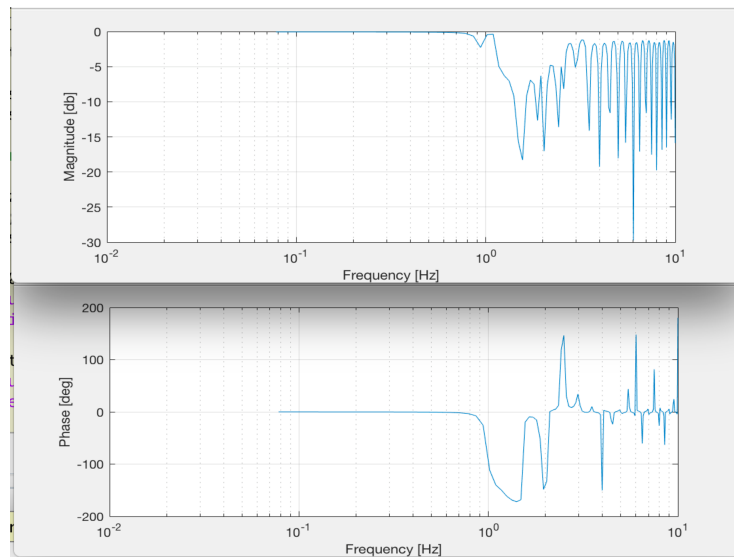
Figure 20. PID automatically tuned controller frequency response
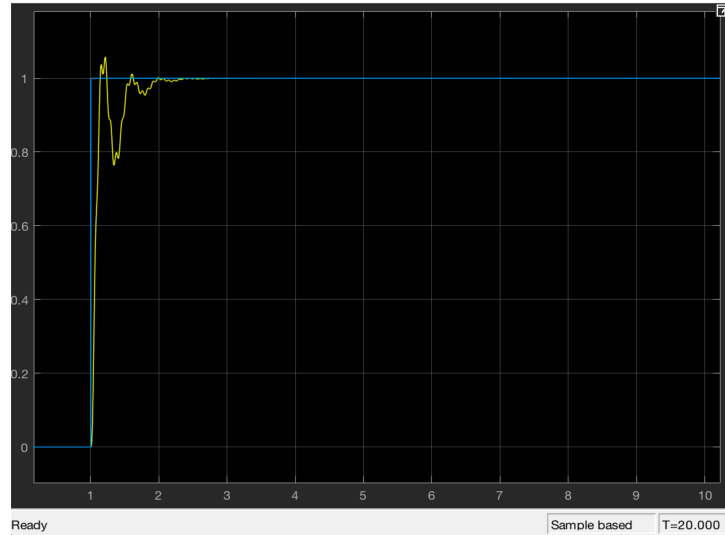
Figure 21. Auto-tuning PID block diagram controller

From the above pictures, the phase and magnitude start exciting to the noisy values around 1.7 Hz.

And the settling time in the time response is around 2.7 seconds.

4-1-2 PID with derivative in feedback loop

The second one, can be the numeric method that, the coefficients of P, I and D should be determined step by step in MATLAB M file. First, the controller with the proportional strategy and unit feedback is assumed as figure 18 and formula 22.

The proportional control strategy is that in the first step put the $T_i \rightarrow \infty$ and $T_d \rightarrow 0$ for different values of K_p the closed loop response of the system will be obtained as figure 22and 23.
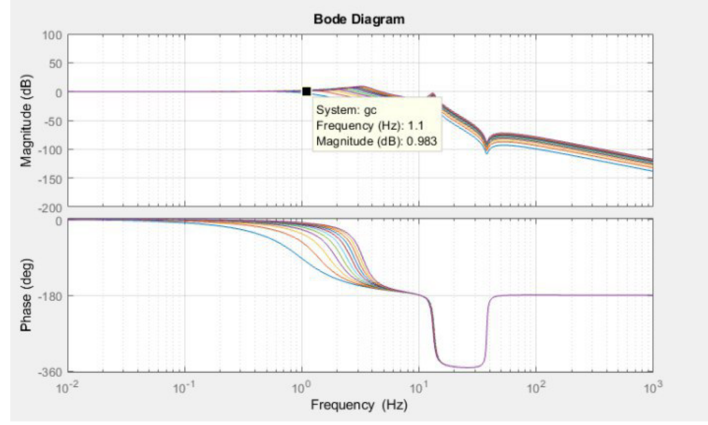
Figure 22 PID numerical tuning to *find and choosing best* K_p
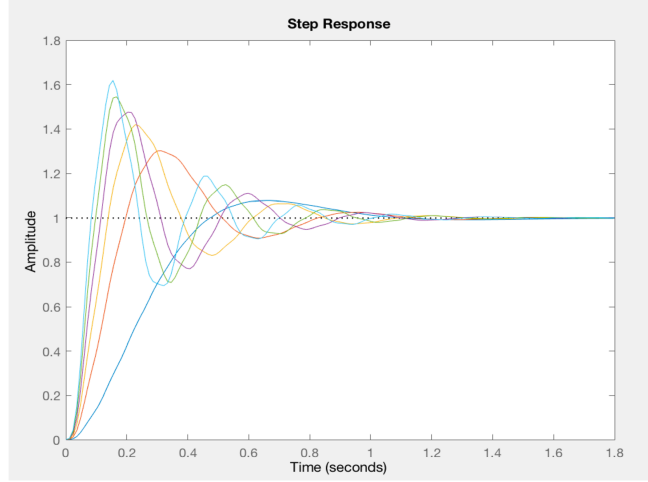
Figure 23. step response to find best *t* K_p for controller with unit feedback

It can be seen, the speed response, overshoot and the steady state error are changed; by increasing the K_p from 0.1 to 1.1 we have fast but unstable result, but also the stable result of the $K_p = 0.1$ will be settle in 1.2 seconds which is acceptable for this thesis goal. Here the best K_p is chosen 0.1. For the next step, $K_p = 0.1$ is fixed and PI control strategy is applied to see the closed-loop response for different T_i as figure 24 and 25.
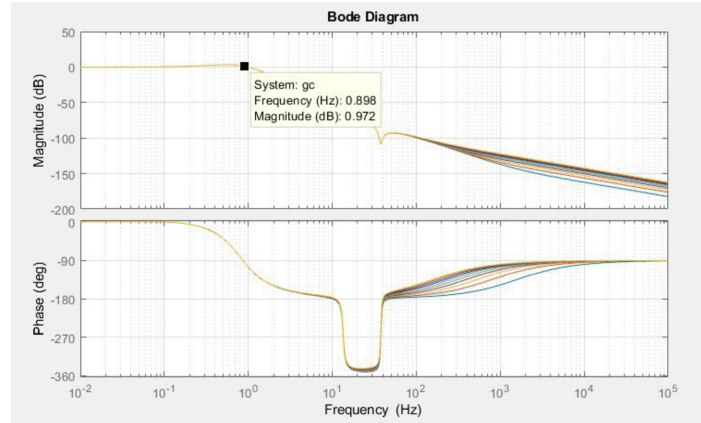
Figure 24. PID numerical tuning to find and choosing best T_i
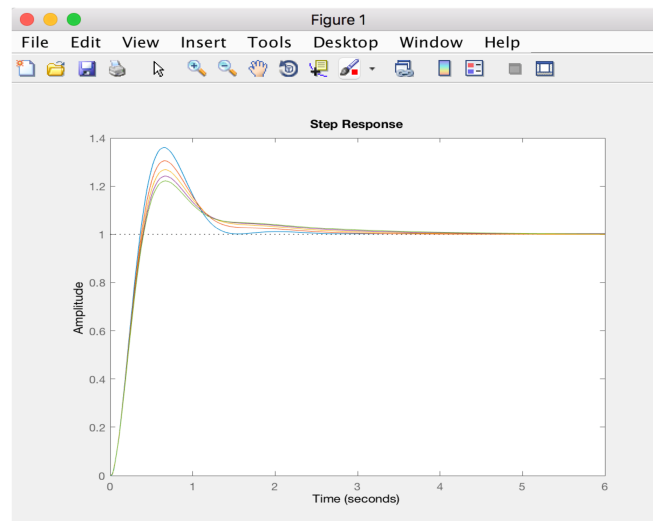
Figure 25. step response to find best T_i for the PID controller with unit feedback

By increasing the T_i from 0.7 to 1.5, system has less over shoot but the settling time become more.

So, the best T_i will be 0.7.

To find the last coefficient, T_d, the closed-loop response with certain K_p and T_i in the period of [0.0001,0.001] will be shown in figure 26 and 27. Which all the T_i in this period have tiny difference but the best answer will be 0.0001.
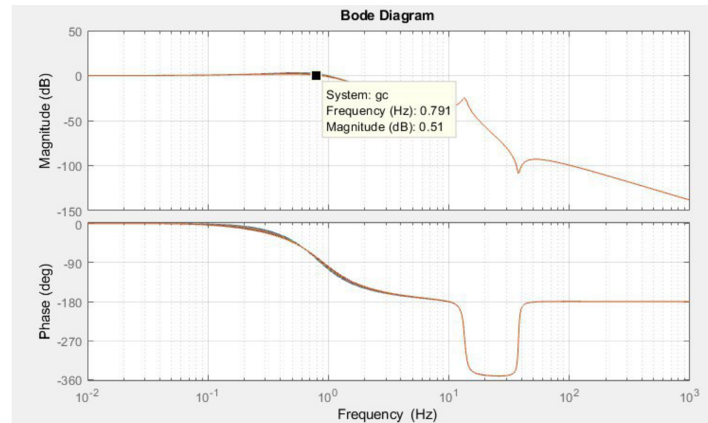
Figure 26. PID numerical tuning to find and choosing best T_d
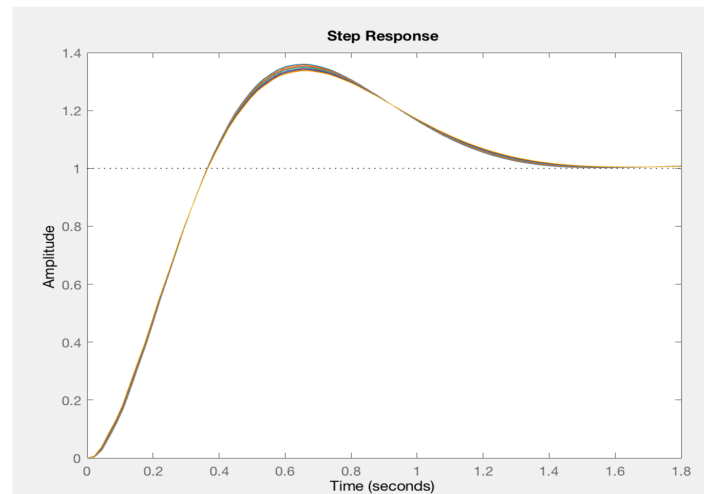
Figure 27. step response to find T_d of the unit feedback PID controller

In each step of finding the coefficients the best answer is going to be chose which is closer to 1 Hz frequency.

For the practical use of PID the pure derivative action is never applied because of the derivative kick produced in control signal while we have the step input and the undesirable noise amplification. The solution can be a first-order low-pass filter. So, the control input in Laplace transforms into a new formula:

$$u(t) = K_p(1 + \frac{1}{T_i s} + \frac{sT_d}{1+s\frac{T_d}{N}}) \qquad (22)$$

the coefficient N could be any number between 1,10,100,1000 but here it is better to use N=1 because it is directly affecting the simulation time.
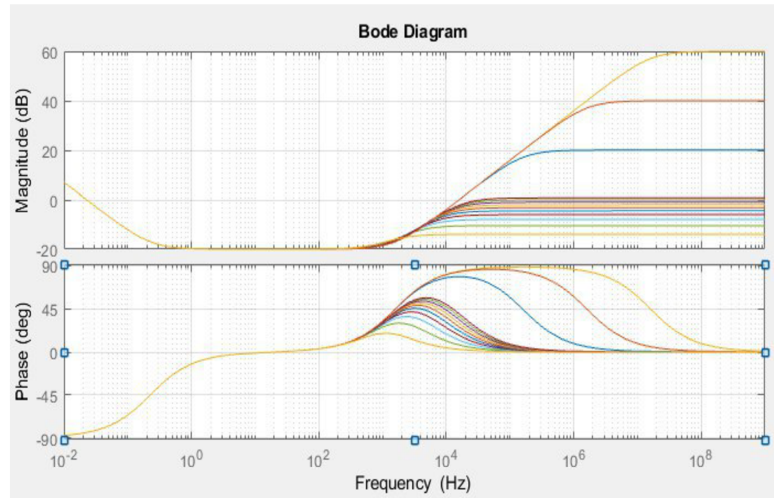
Figure 28. mistaken frequency response of the system with unit feedback to eliminate the derivative kick

From the above figure it shows that, there is a jump around 0.98 Hz which is an error that means the derivative action may not be desirable in such a control strategy. So, it is better to put the derivative term in the feedback path.
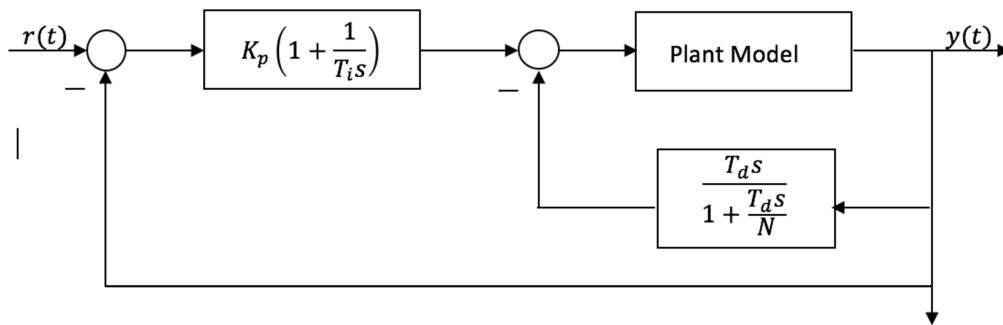
Figure 29. PID controller with derivative on output signal

N, is a coefficient which can be a number between 1, 100,100,1000. In my model, it is better to put N=0.1.

The final result of time and frequency response will be as bellow:
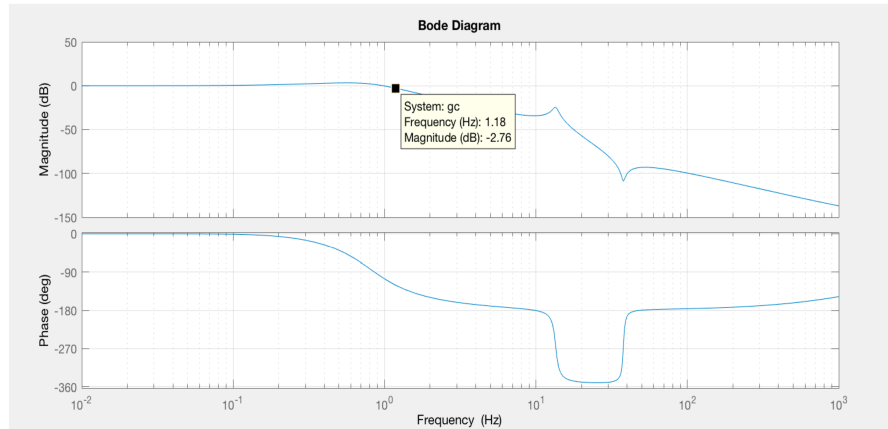
Figure 30. frequency response of the steering wheel angle position controlled by PID
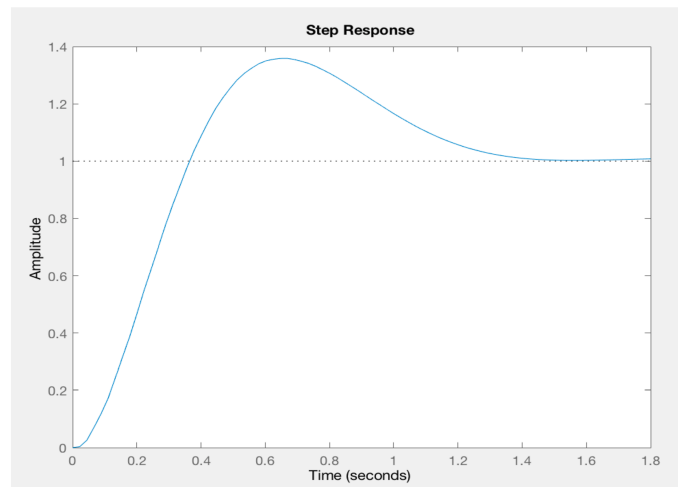
Figure 31.step response of PID controller with derivative feedback loop

It seems that the PID controller works correctly and has the corresponding result of 1.18 Hz than expected. In the bode diagram, the behavior of the system between 10 to 50 Hz which has the sudden decrease and peak, is because of the resonance frequency of the whole system which causes very low magnitude.

4-2 MPC simulated results

On the other hand, as a third controller, MPC block in Simulink can be used.

Model predictive control uses linear plant, disturbance and noise models to estimate controller state and predict future plant outputs. Using the predicted plant outputs, the controller solves a quadratic programming optimization problem to determine optimal manipulated variable adjustments.
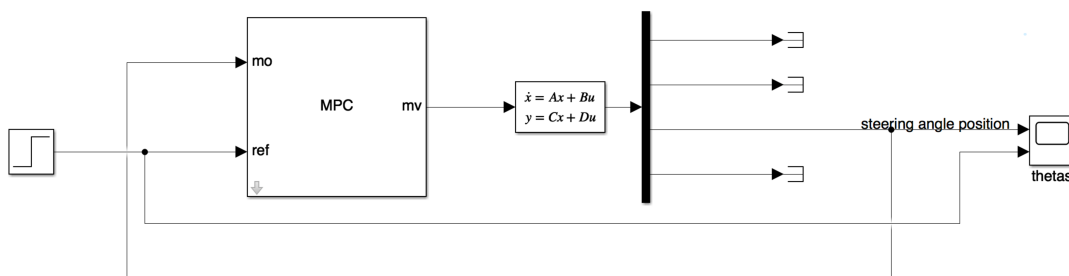

Figure 32. MPC controller block diagram

The responses of the controlled steering angle position with MPC block are shown as bellow.
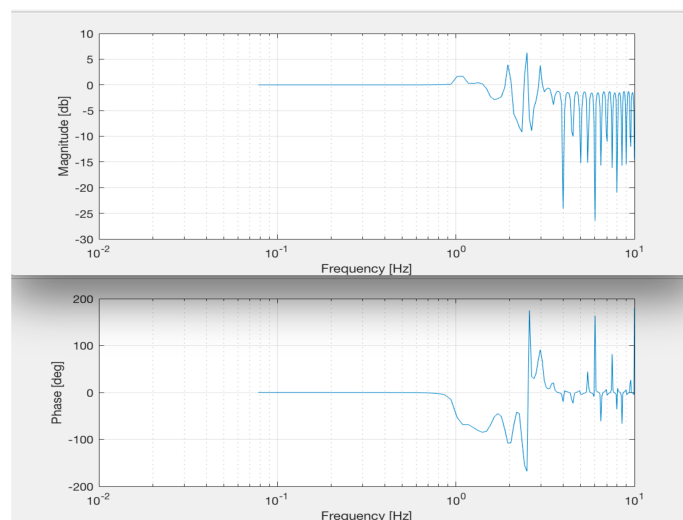
Figure 33. frequency response of steering angle position controlled by MPC block by ideal step input
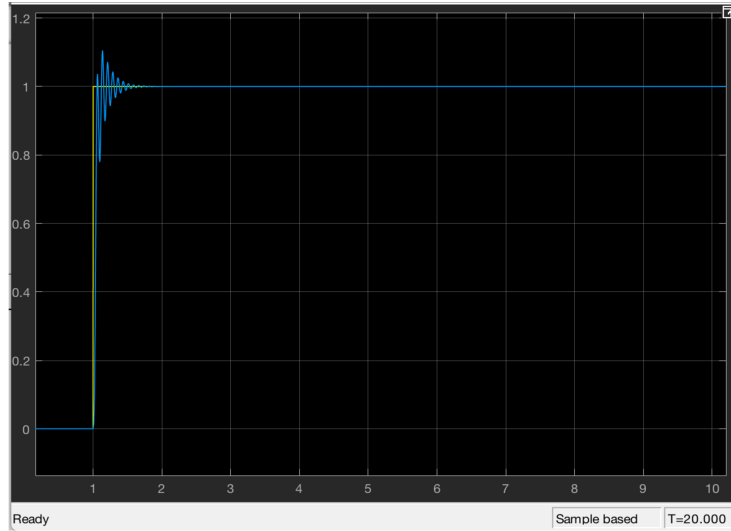
Figure 34. step response of the EPS with MPC controller

So, the MPC block can have also good results of the ideal condition with step input, which is reached stable respond after 0.5 second with fast answer. In the bode diagram of figure 33 also the system is excited the magnitude and phase of the system between 0.9 and 2.5 Hz frequency.

5. Linear model responses:

To test the general EPS modelling and different control strategy until now, the responses of the total system were with respect to the step input. but to reach the goal of testing the model in a non-linear environment, it is necessary to test the best linear models with respect to the Carmaker lateral dynamics inputs which are sinus and sinus sweep, sinusoidal and chirp input signals are considered as linear inputs to have equal condition in linear and non-linear model comparison.

For each control strategy, there are four responses of time and frequency for 2 different inputs. The sinusoidal input with the amplitude of 1 and the frequency of 1.255 rad/sec. And the chirp

signal to have sinusoidal behavior with stationary amplitude and variable frequency in time with

initial and target frequency of 0 to 10 Hz and amplitude of 1 as bellow:
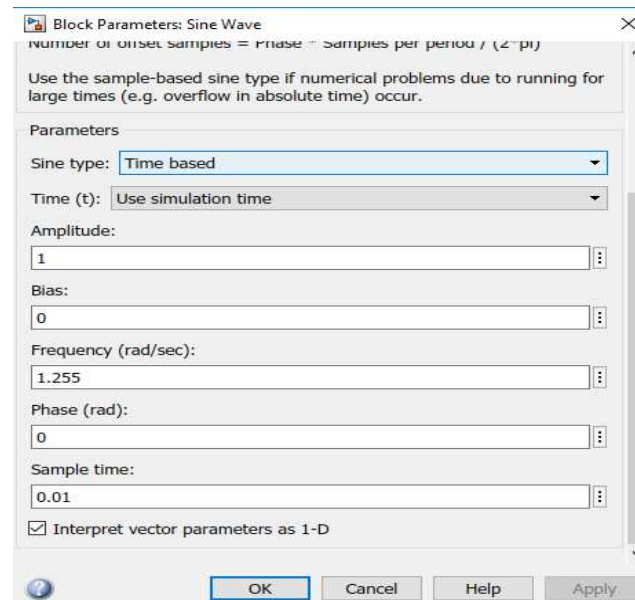

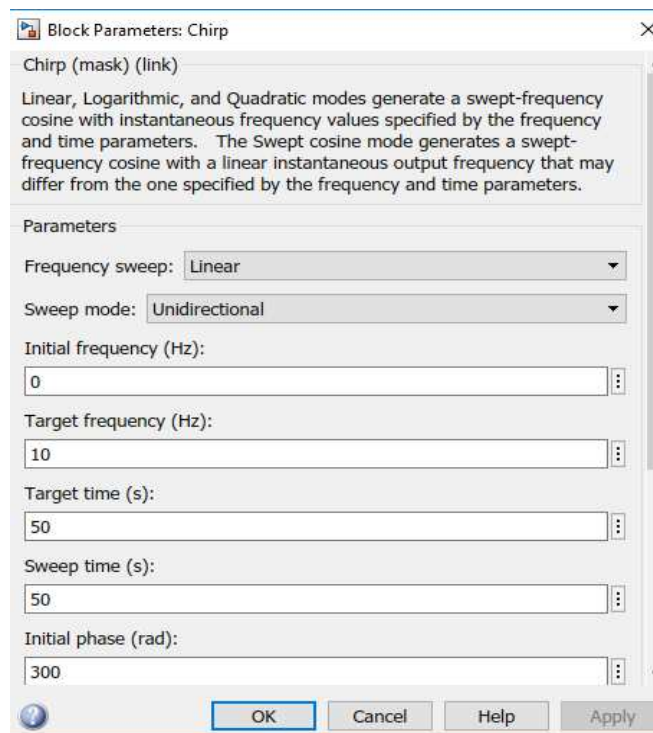Figure 35. sinusoidal input regulation of the linear EPS model

Figure 36. chirp signal input regulation of the linear EPS model
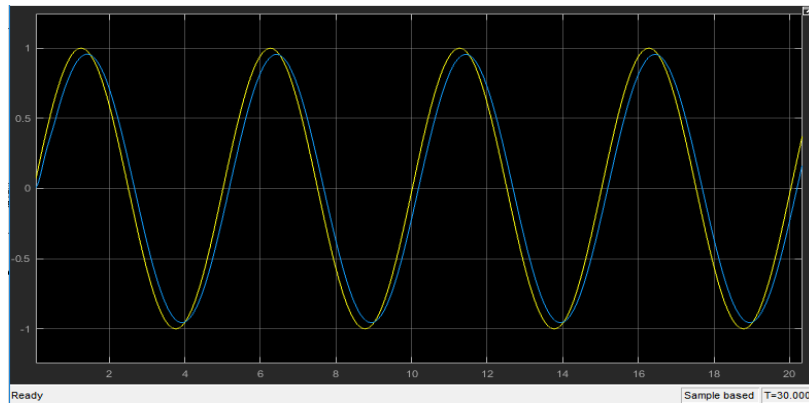
Auto-tuning PID:

Sinusoidal input:

Figure 37. time response of the Auto-tuned PID with respect to the sin input

Figure above shows 0.03 difference in amplitude and 0.15 time delay between the input and the

model result.
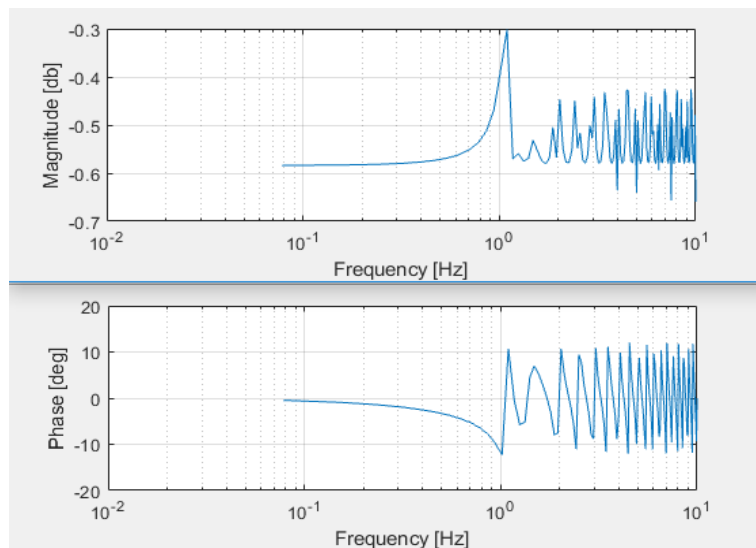
Figure 38. bode diagram of the Auto-tuned PID with respect to the sin input

Bode diagram illustrate that the magnitude start changing from -0.5 dB increase to -0.3 dB and

again decrease in -0.57 dB in period of [0.7, 1.09,1.17] Hz after that noises appear. Phase also

starts from 0 degree to -12.29 increase to 10.67 and decrease in -5.21degree respectively in 1.01, 1.09 and 1.32 Hz.
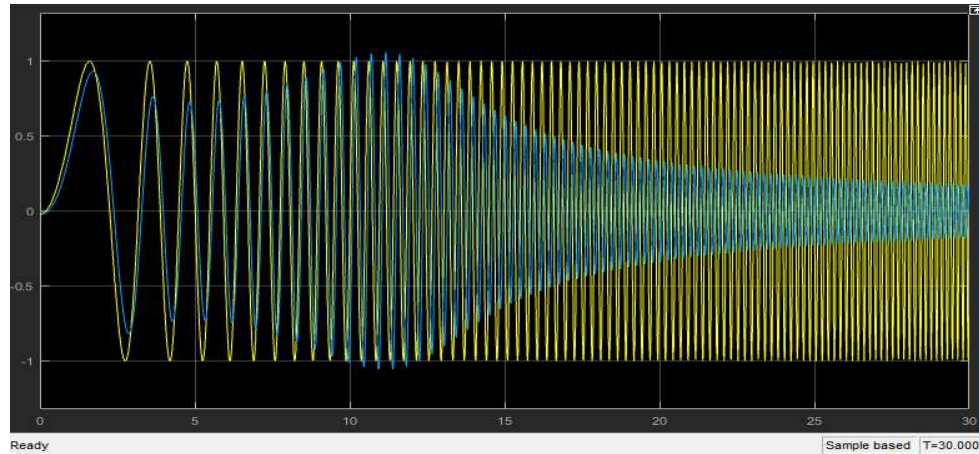
Chirp input signal:

Figure 39. time response of the Auto-tuned PID with respect to the chirp input signal

Time response amplitude is decreased from 0 to 5 seconds then increased in following 7 seconds and again decrease from 12 second to the end which means that at very high frequency amplitude goes to 0. Also, the time delay is about 0.2.
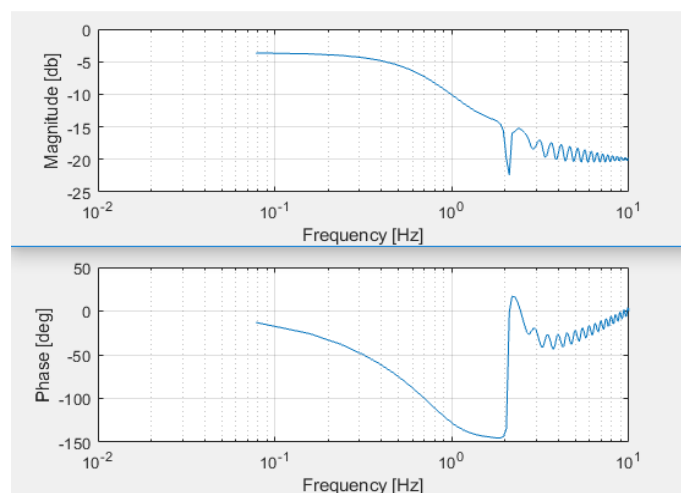

Figure 40. frequency response of the Auto-tuned PID with respect to the chirp input signal

The bode diagram shows magnitude changes from -3.6 dB to -22.4 dB and -15.25 in frequency of [0.3, 2.1, 2.4] Hz. And the phase is changed from -13.02 degree to -145.2 and 16.43 degree in [1.79,2.26] Hz frequency.
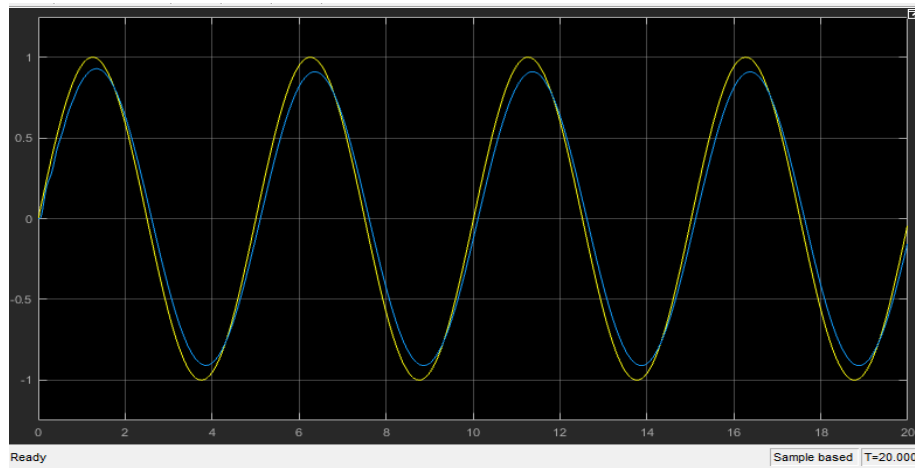
PID with derivative feedback:

Sinusoidal input:

Figure 41. time response of the PID with derivative feedback with respect to the sin input

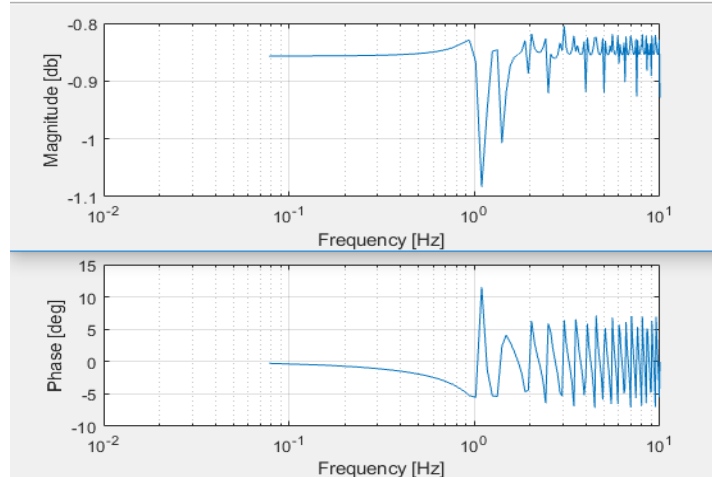Figure 41 shows, 0.09 difference in amplitude and 0.1 delay between the input and the model result.

Figure 42. bode diagram of the PID with derivative feedback with respect to the sin input

Bode diagram in figure 41 shows that the magnitude start changing from -0.85 dB increase to -0.84 dB and again decrease in -1.1 dB in period of [0.7, 1.09] Hz after that noises appear. Phase also starts from 0 degree to -5 increase to 11 degree again in [0.7, 1.09] Hz.
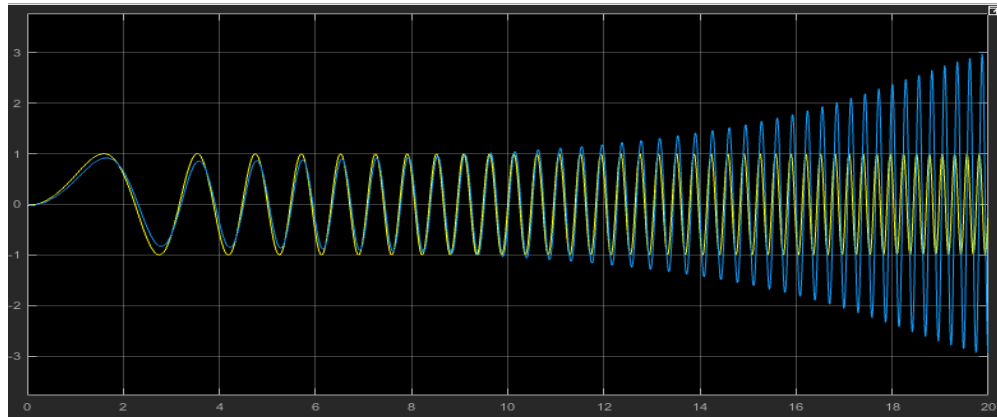
Chirp input signal:

Figure 43. time response of the PID with derivative feedback with respect to the chirp input signal

From figure 43, the result amplitude is stable in first 11 seconds then increase by increasing the input frequency. In stable area, the amplitude difference is 0.15. and it has a little delay of 0.04 in time.
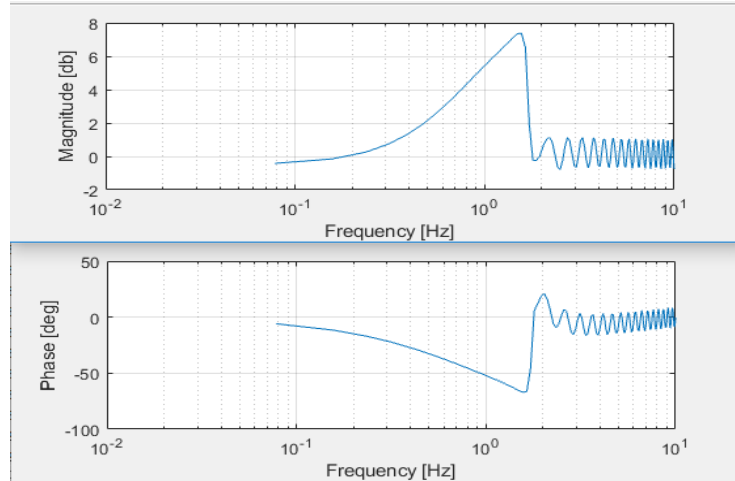
Figure 44.bode diagram of the PID with derivative feedback with respect to the chirp input signal

From the Bode diagram in figure 44, the magnitude start changing from -0.41 dB increase to 7.33 dB and again decrease in -0.24 dB in period of [1.56, 1.7] Hz after that noises appear. Phase also starts from -5.87 degree to -67.07 increase to 21 degree in [1.56, 2.03] Hz.

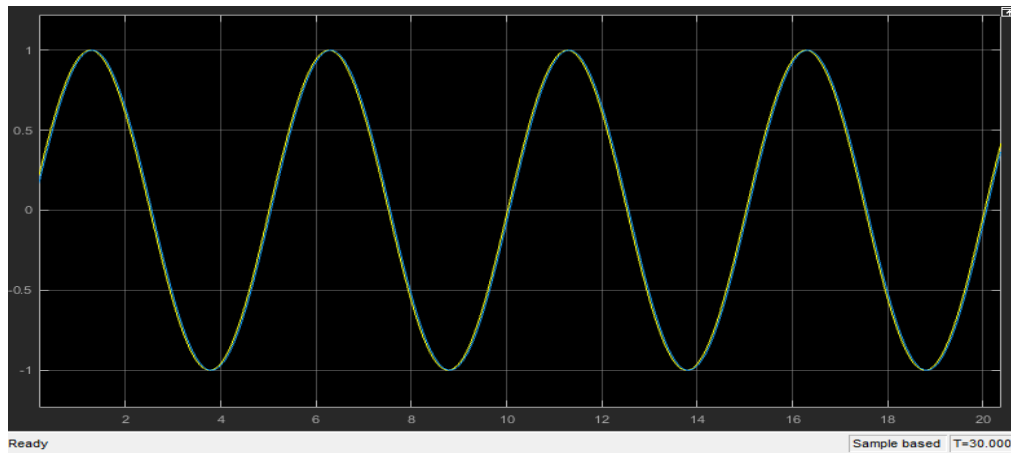**MPC controller**:

Sinusoidal input:

Figure 45. time response of the MPC with respect to the sin input

Figure 45 is the perfect results of time response among controllers which has the same amplitude as input and 0.03 sec delay.
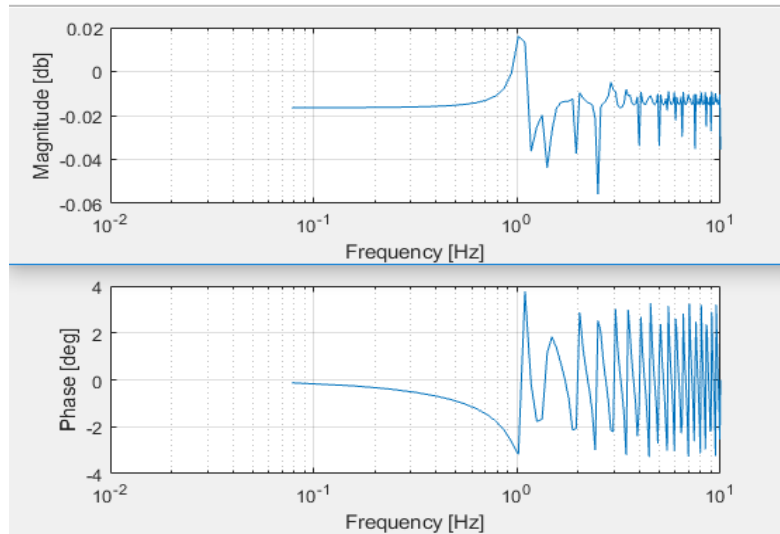
Figure 46. bode diagram of the MPC with respect to the sin input

Its Bode diagram has the magnitude of -0.01 dB at the beginning of change then increase to 0.01

dB and again increase in 0.03 dB in period of [0.06, 1.01, 1.1] Hz before noises appear. Phase also

starts from -0.12 degree to -3.1 increase to 3.7 degree in [1.01, 1.09] Hz.
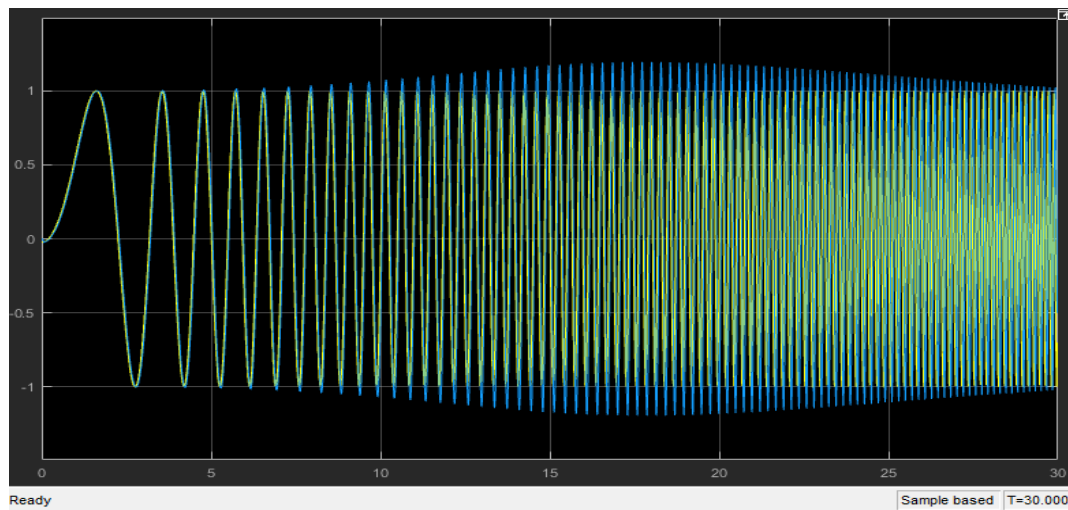
Chirp input signal:

Figure 47. time response of the EPS controlled by MPC with respect to the chirp signal as input

In MPC time response, amplitude is stable in first 7 seconds then increased from 7 to 18 sec and again decrease from 18 to 30 sec which means that at very high frequency amplitude is not stable and become noisy. Also, the time delay is about 0.05.
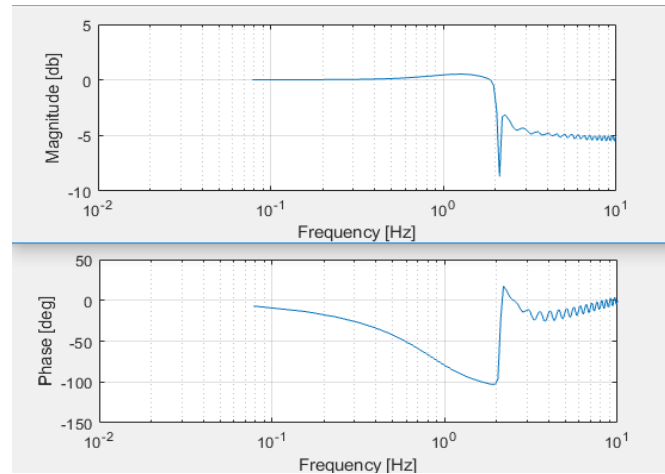

Figure 48. frequency response of the EPS controlled by MPC with respect to the chirp signal as input

In frequency response of figure 48, the magnitude starts from 0 dB at the beginning of change in 0.3 Hz then increase to 0.4 dB in 1.4 Hz and decrease in -8.6 dB in 2.1 Hz and finally increase by -3.3 dB in 2.1 Hz. Phase also starts from -6.9 degree to -102.9 increase to 17.6 degree and decrease by -13.8 in frequency period of [1.87, 2.1,2.8] Hz.

6. IPG CarMaker simulation

CarMaker is a software produced by company IPG automotive, aimed to simulate the vehicle dynamic of the four-wheeled passenger cars based on mathematics for modeling the Virtual Vehicle Environment (VVE). VVE specify the characteristics of vehicle, driver and road simulation by detail. So, it provides all parts required to evaluate a controller designed to test a vehicle subsystem.

6-1 simulation method

In the next step of thesis with the acceptable results of the controller, the Simulink model should be added to the real model of the vehicle in IPG Carmaker software.

The IPG Carmaker projects should be opened in MATLAB current folder and the assumption model of the vehicle should be chosen by its parameters in detail.

In the generic model of Carmaker which can be opened through MATLAB, there is a vehicle model with all blocks of the different part of the vehicle.

CarMaker 6.0.5

Generic Car Model

You may use this model as a starting point.
It already contains everything to run a simple CarMaker simulation.
Build your Simulink model around it.
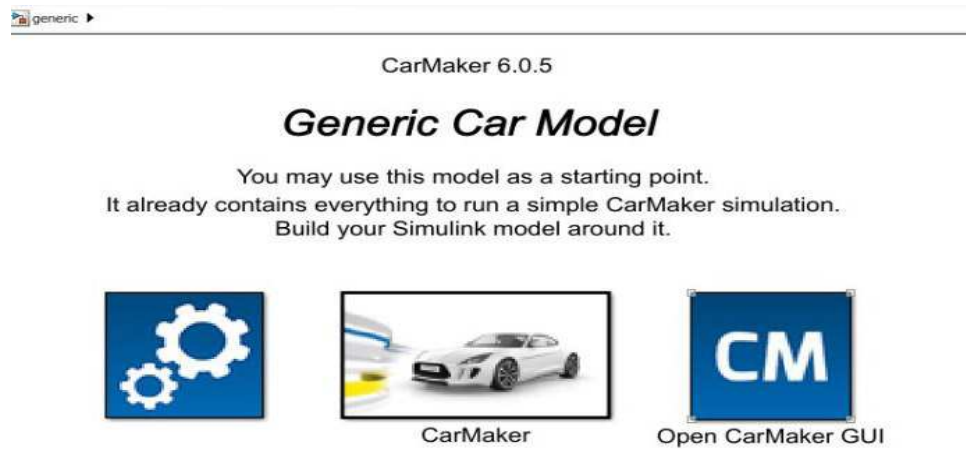
CarMaker

Open CarMaker GUI
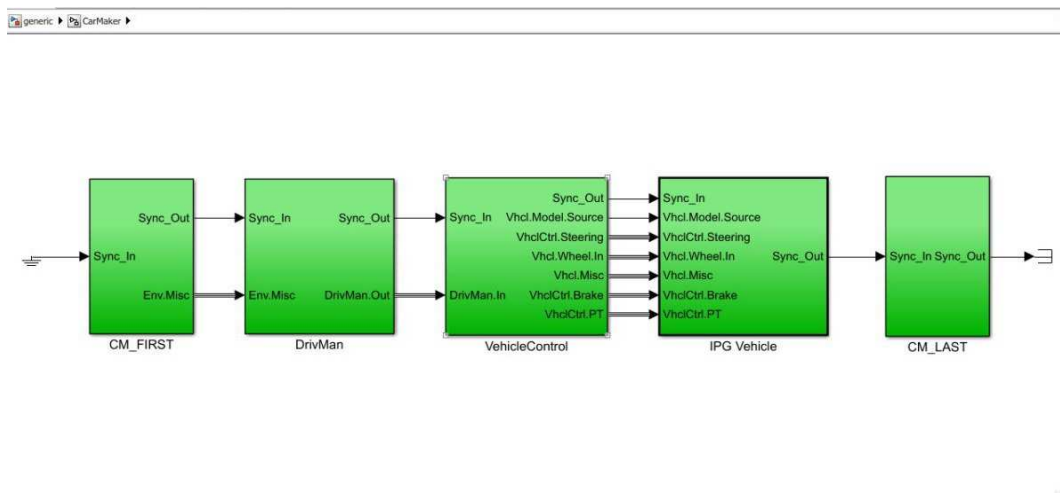
Figure 49. generic CarMaker model

Figure 50. CarMaker vehicle simulation block

As figure 50, the first block, CM-First, is an initializing block to read or write any value or constant parameter definition. The next block is DriveMan, which means to do the driving manager as different scenarios and maneuvers. In vehicle control block as the third one, is the main block which a lot of automotive researches and tests have been done here as model the EPS system or to add different kinds of custom made controllers and the most accessible and changeable one. In

IPG vehicle block there is physical model available here specifically the car end trailer and break and power train that each one has subsystem of specific signals related to the physical aspect of the vehicle. The block also for initializing the value which is initialized at first block and tune them. So, the model of the steering column and the control part should be added to the prepared model of Carmaker through the vehicle control block.

For adding the designed EPS model and controller to the CarMaker, inside the vehicle control block between to vehicle control function block there is a sub system of controller busses which the input steering reference angle and the action output busses can be find. The the model should be added between this two busses as figure 51.
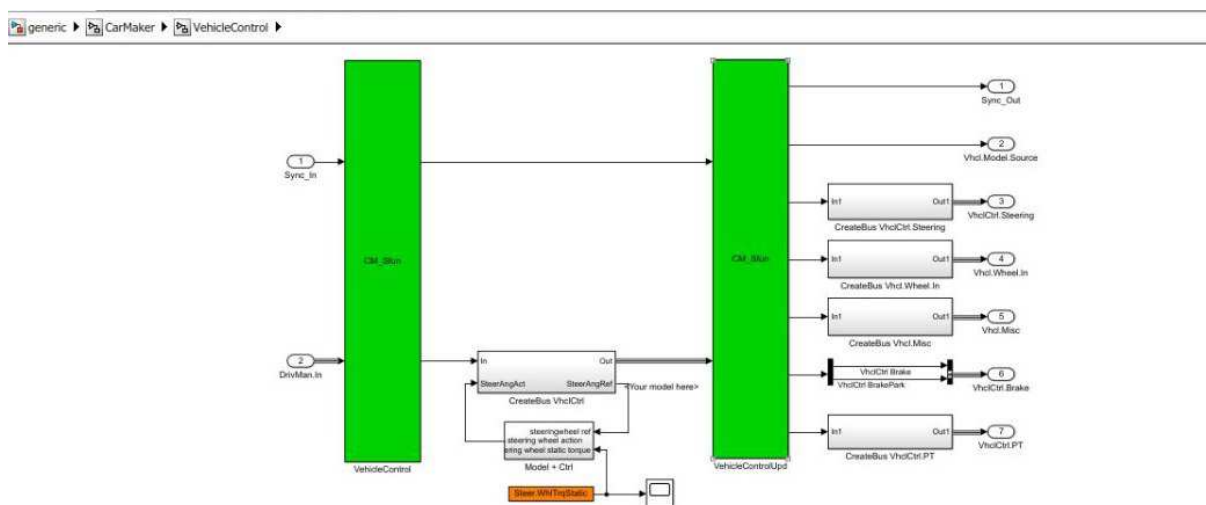

Figure 51. connected EPS and controller model between input and output of the vehicle steering angle ports

Meanwhile, to add the driver steering torque to the upper part of the EPS model (steering part), steering wheel torque static block from the CarMaker library can be chosen.

By running the whole simulation, the IPG setup parameters page will be opened. A demo compact passenger vehicle is chosen which has the predefinition of different real vehicle parameters as tire,

road, sensors, body and trailer in a specific road scenario which can be defined by user and the maneuver of 10 Km/h speed and the input motor torque of IPG driver, sinusoidal and sinus sweep. Each of the vehicle parameters can be regulated and changed for specific car but here a simple general demo model has been chosen to see the designed model validation in real vehicle model.
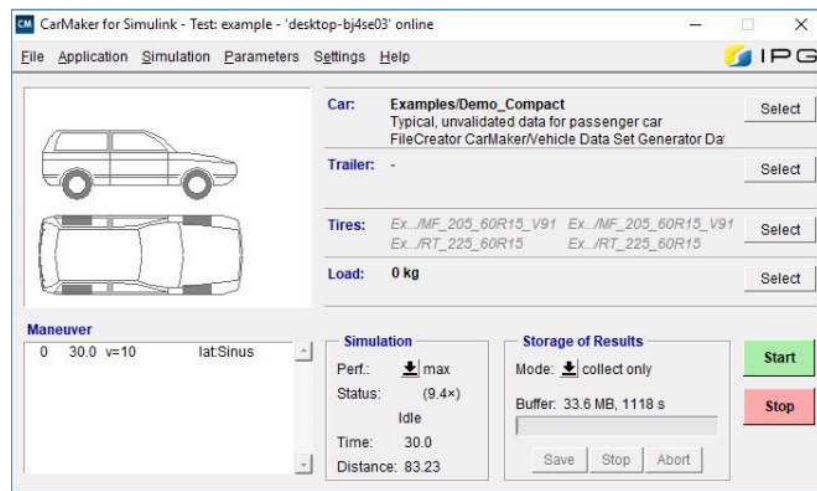

Figure 52. setup vehicle parameters in IPG CarMaker

Inputs of CarMaker can be changed in sinosiodal and sinus sweep in maneuver part as bellow which are approximately equal to the inputs chosen for the linear analyse of the EPS model. The sinus input with amplitude around 1 and period of 5 seconds. And the sinus sweep by the exact amplitude of 1 (57 deg) and period of 5 sec to 0.005 sec variable.

Figure 53. sinus input set out in IPG CarMaker maneuver

Figure 54. sinus sweep input set out in IPG CarMaker maneuver

If considering the system without any controller, can be seen that the results is not much precise and there is a waste of half amplitude in input and output signals.
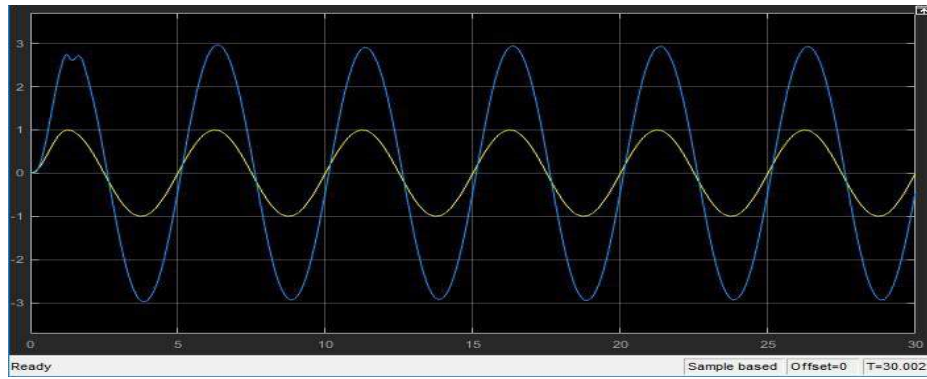
Figure 55. time response of the system in carmaker non-linear area without any controller
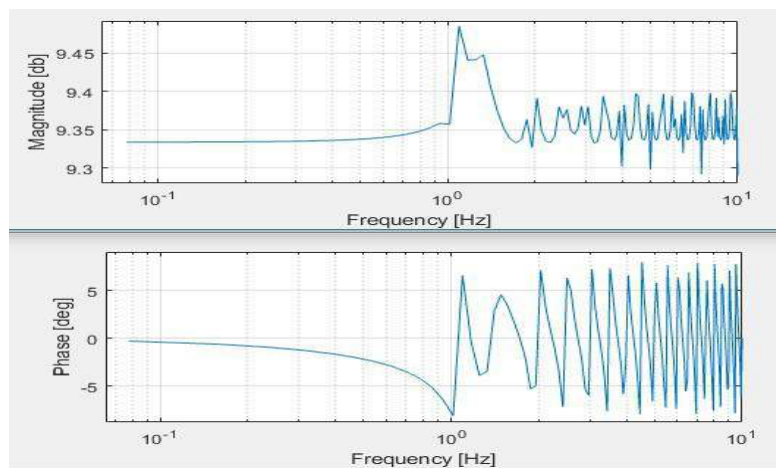

Figure 56. bode diagram of the system in carmaker non-linear area without any controller

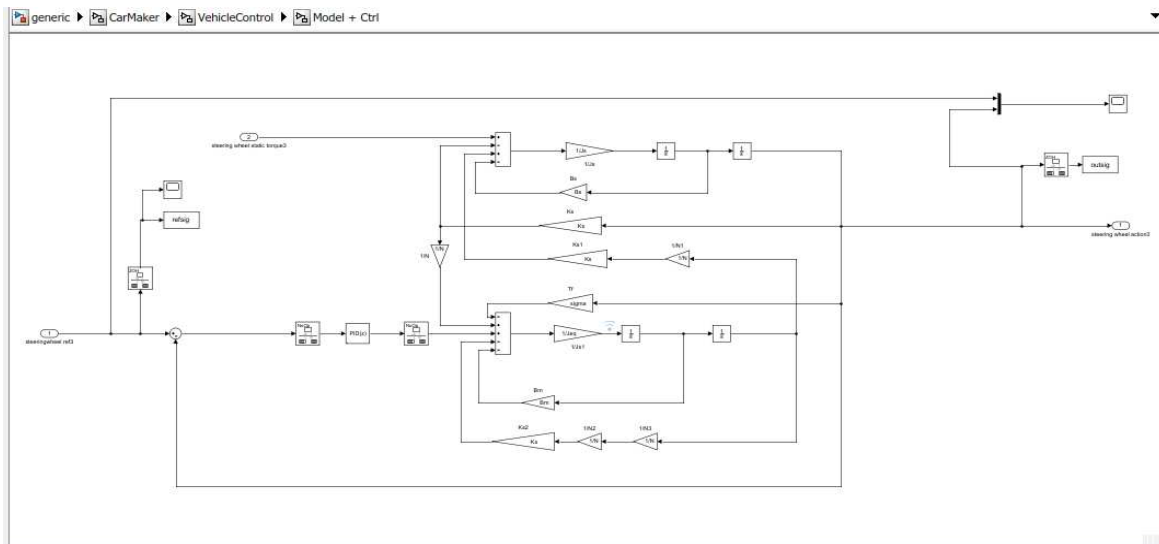**Auto-PID nonlinear analysis:**

Figure 57. Auto-tuning PID model in CarMaker vehicle modeling
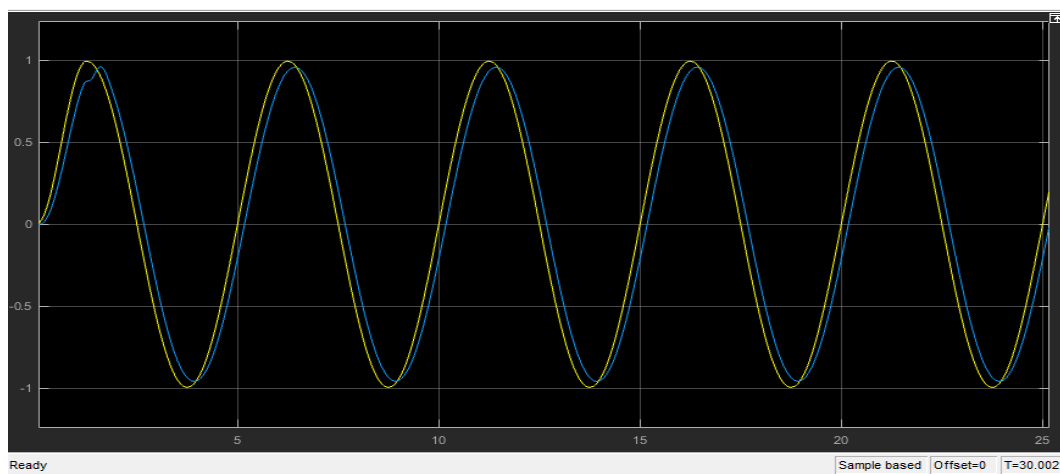
Sinus input:

Figure 58. time response of the EPS model controlled by Auto-tuned PID in nonlinear area with respect to sinus input

Figure above shows that the nonlinear plot result has about 0.03 difference in amplitude and 0.15 sec time delay.
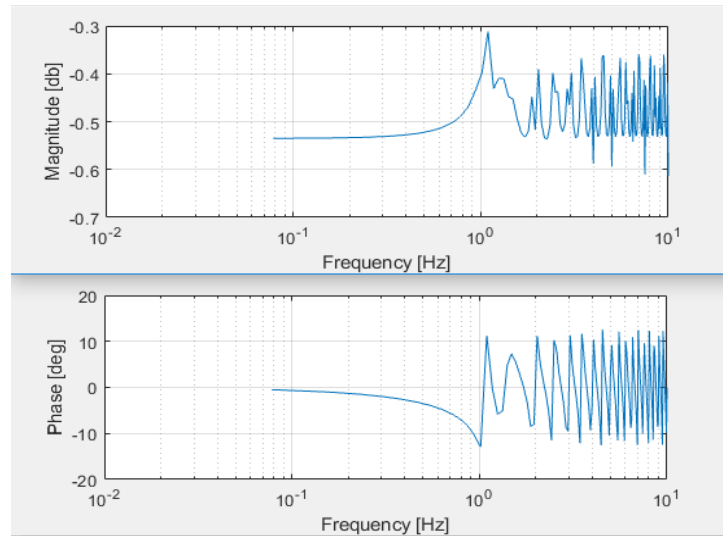
Figure 59. bode diagram of EPS controlled by Auto-tuned PID in nonlinear area with respect to sinus input

Also, its frequency response illustrate the magnitude is differ from -0.53 to 0.31 and -0.53 dB from 0.7 Hz to 1.172 Hz frequency. In addition, phase is changed from 0 to -12.94 and +11.292 degree and again in -5.8 at 1.25 Hz max frequency.

Sinus sweep input :

Figure 60. time response of the EPS model controlled by Auto-tuned PID in nonlinear area with respect to sinus sweep input

In figure 60 the amplitude is slightly decrease in 11 seconds, increase between 11 and 13 sec and then decrease until 18sec, increase little during 4 seconds and at the end lead to 0 which means instability in high frequency. In addition, there is an approximate of 0.1 of time delay.
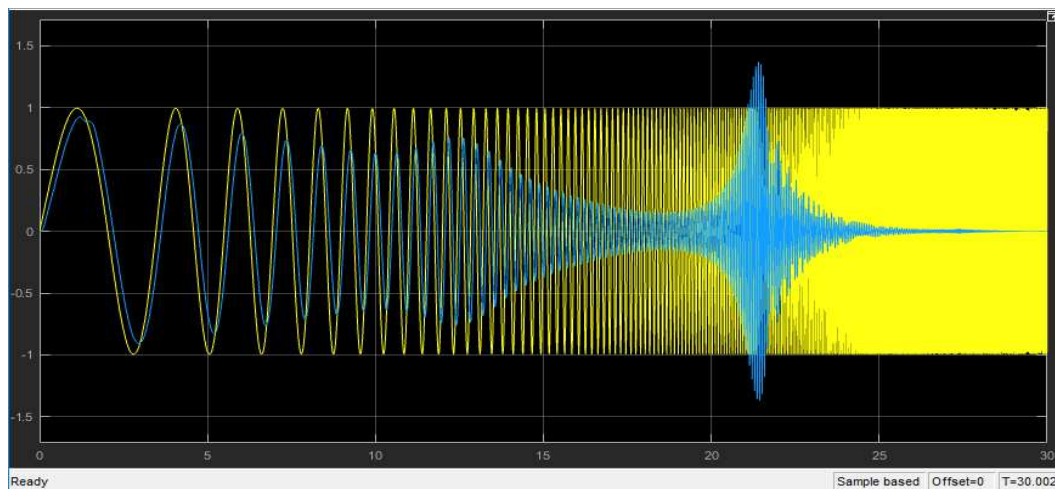

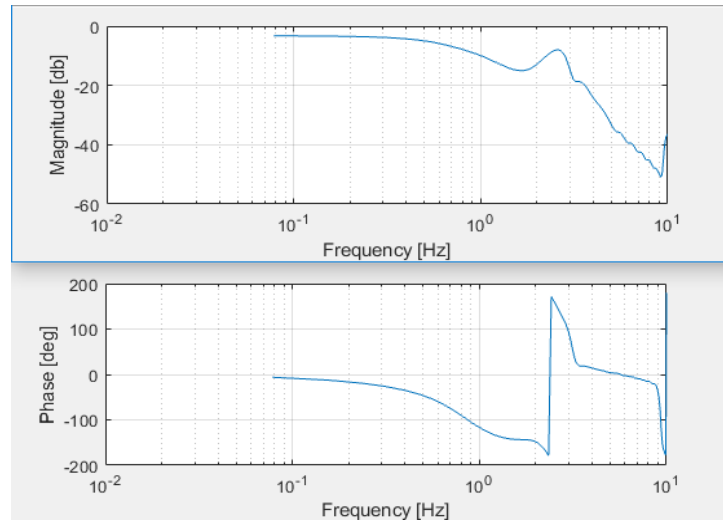Figure 61. bode diagram of EPS controlled by Auto-tuned PID in nonlinear area with respect to sinus seep input

Bode graph in figure 61 has the magnitude of -3.2 dB at first, decrease to -15.02 dB and increase to -7.9 in 0.4, 2.3 and 2.4 Hz frequency respectively. The phase of the system is varied from 0 to -143 degree then 171.7 degree and 21.25 degree before the noisy behavior in the frequency period of [1.56, 3.3] Hz.

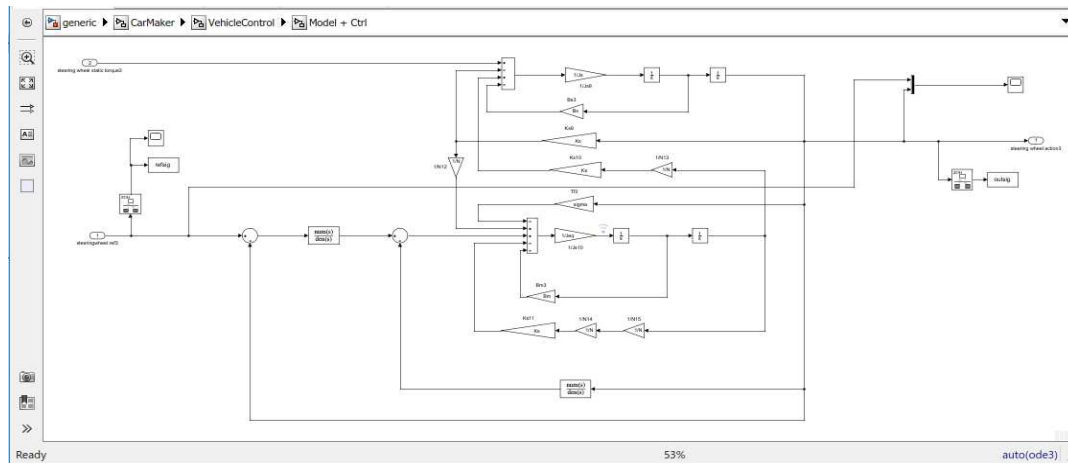**Nonlinear Model with PID controller with derivative feedback:**

Figure 62. EPS model controlled by PID with derivative in feedback in nonlinear environment of CarMaker
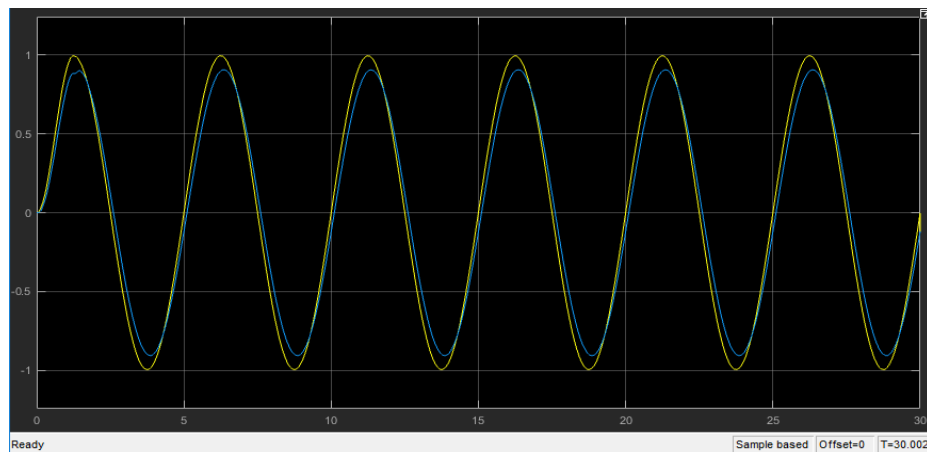
Sinus input:

Figure 63. time response of the EPS model controlled by PID with derivative feedback in nonlinear area with respect to sinus input

Nonlinear model time plot of figure 63 shows 0.09 difference in amplitude and 0.1 delay in time.

Figure 64. bode diagram of EPS controlled by PID with derivative feedback in nonlinear area with respect to sinus input

Frequency response of nonlinear system by PID controller with derivative feedback in figure 64, have the magnitude of -0.87 increase in -0.81 and then decrease at -0.89 in the period of 0.7 to 1.172 Hz frequency. The phase also decrease at first from 0 to -7 degree then increase equally to +7 at the max frequency of 1.09 Hz.

Sin sweep input:

Figure 65. time response of the EPS model controlled by PID with derivative feedback in nonlinear area with respect to sinus sweep input

In time response of figure 65, amplitude is stable in first12 seconds which has the low frequency at the beginning and the amplitude in this period has 0.14 difference from the input signal, then the amplitude increased from 12 to 15 second and again decrease to the end. Also, the time delay is about 0.05.
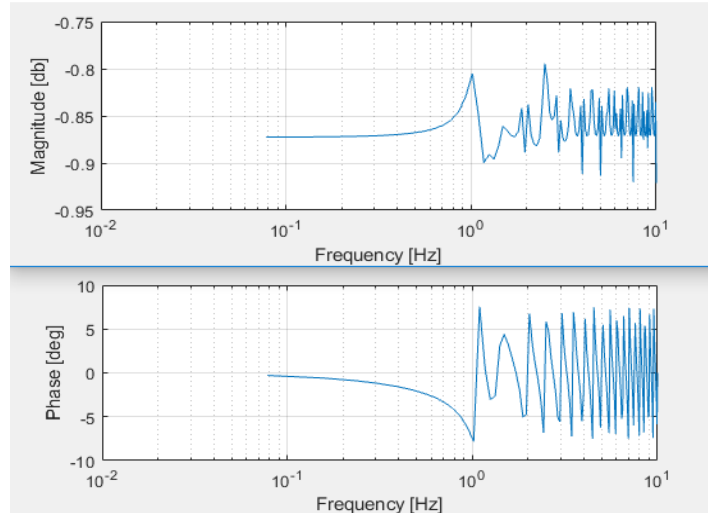

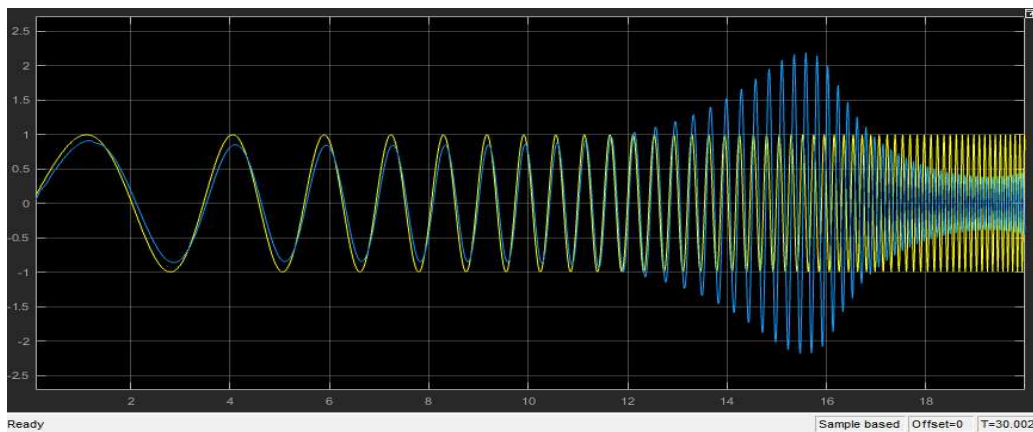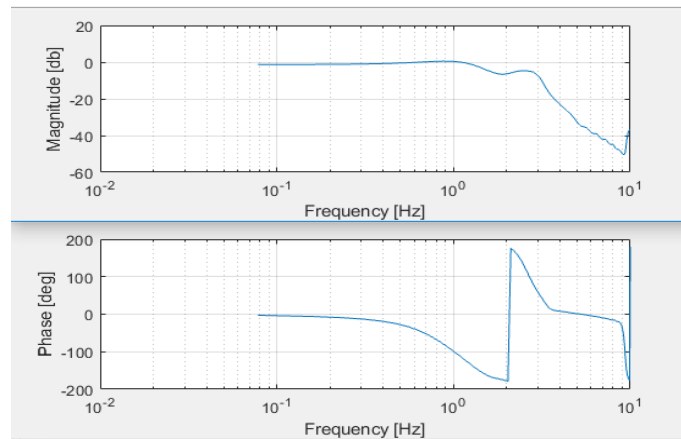
Figure 66. bode diagram of EPS controlled by PID with derivative feedback in nonlinear area with respect to sinus sweep input

In the bode diagram of above, magnitude is increased from -1 dB to 0.5 then decrease to -6 dB in the period of [0.5, 2.5] Hz. And phase is changed from 0 to -176 degree and increase equally to +176 degree and 11 at the end in the frequency of 0.3, 2.03, 2.1 and 3.5 Hz.

MPC controller for the model in nonlinear area:
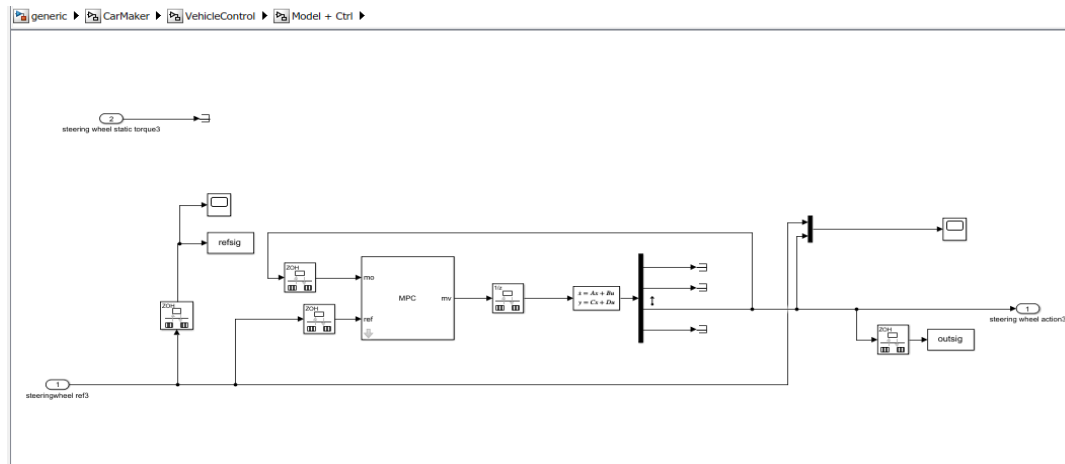
Figure 67. EPS model controlled by MPC block in nonlinear environment of CarMaker
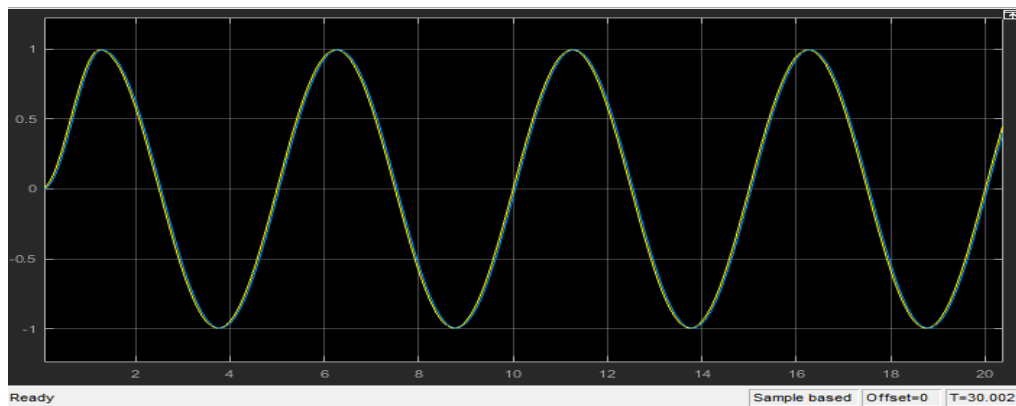
Sinus input:

Figure 68. *time response of the EPS model controlled by MPC in nonlinear area with respect to sinus input*

MPC again shows perfect plot in figure 66 as the linear result which has the same amplitude and around 0.04 delay with respect to the input.
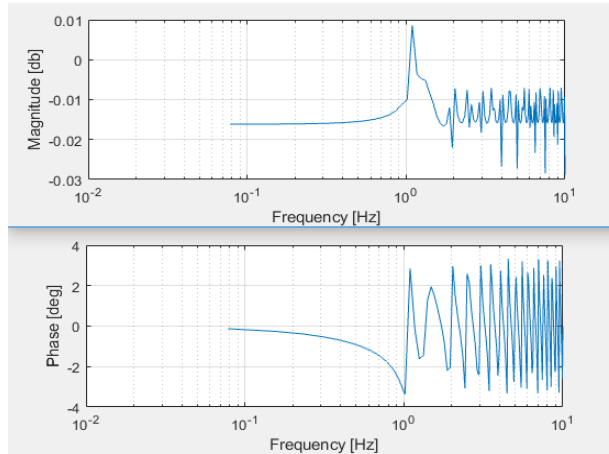
Figure 69. bode diagram of EPS controlled by MPC in nonlinear area with respect to sinus input

Also, figure 69 shows, the magnitude is changed from 0.4 Hz in -0.1 dB to +0.008 and -0.01 dB

in 1.09 Hz and 1.4Hz respectively. and the phase is changed from -0.1 to -3.38 and 2.85 degree in

the frequency of 1.01 Hz and maximum 1.09 Hz.

Sinus sweep input:
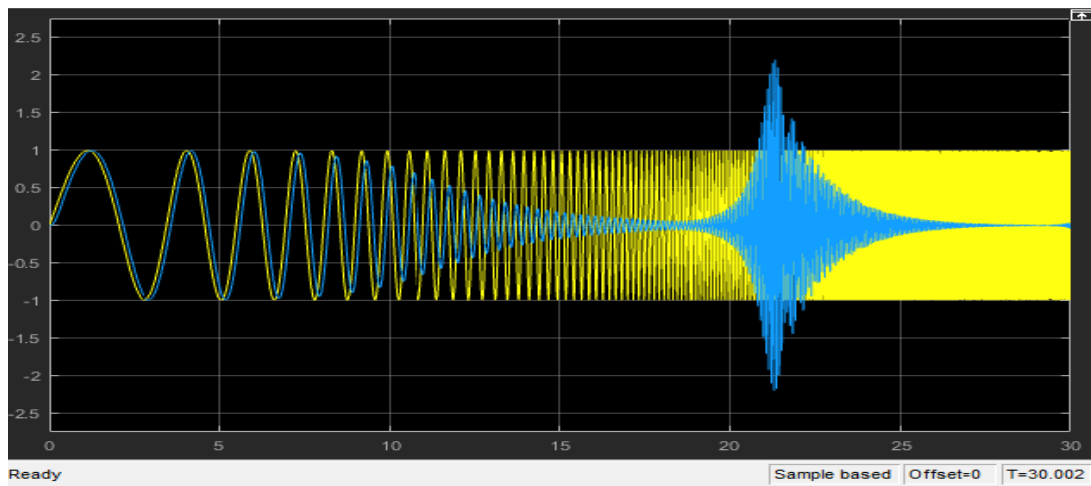
Figure 70. time response of the EPS model controlled by MPC block in nonlinear area with respect to
sinus sweep input

In time response of figure 70, the amplitude remains stable for 7 seconds then decrease in following 11 seconds and increase a little until 22sec and in the very high frequency leads to 0. The resulted graph only has 0.14sec delay with respect to the input.

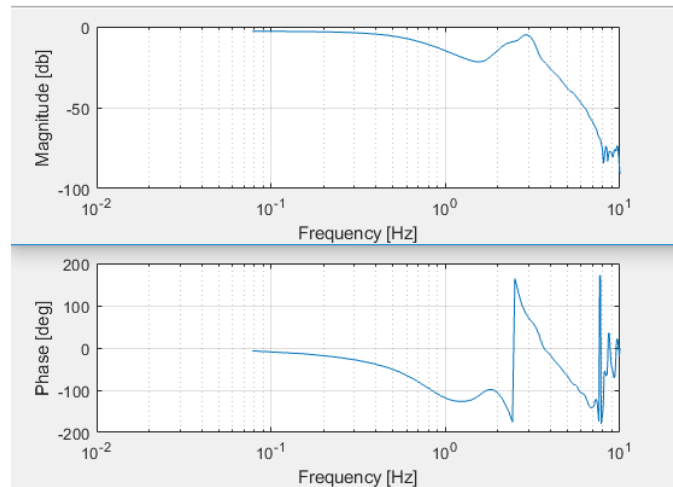Figure 71. bode diagram of EPS controlled by MPC block in nonlinear area with respect to sinus sweep input

Frequency response shows the magnitude start changinging from 0.3 Hz in 0 to -21.5 dB then increase to -5.008 dB in frequency of 1.4 and 1.8 Hz. Phase also changed in the period of [1.25, 2.5] Hz from 0 to -126.8deg and -98.12deg then -175.5 to 164.4 degree.

7. Results comparison:

To conclude and summarize the simulation results, there are plenty of graphs together in one plot available for better realizing the difference between different controllers used in this thesis and the difference between the results with linear and non-linear friction applied to the model and controller. For this purpose, responses changes in frequency domain are more sensitive as compared to time domain.

First, in linear friction application with sinusoidal input as motor torque, for all three controllers, it can be seen, the frequency response of the MPC controller in the same frequency period, has less oscillation in magnitude and phase. After that the PID with derivative feedback has better oscillation than Auto-tuned PID.

Figure 72. bode diagram to compare 3 controllers as green one is MPC, blue one is PID with derivative feedback and red one is auto-tuned PID in linear condition with sinusoidal input

In the same situation but different input as sinus sweep, PID controller with derivative feedback has less phase shift but from the magnitude point of view MPC block has better response; As figure bellow:

Figure 73. bode diagram to compare 3 controllers as green one is MPC, blue one is PID with derivative feedback and red one is auto-tuned PID in linear condition with sinus-sweep input

Second, in non-linear friction condition, when there is sinusoidal input available for motor part, among three controllers, MPC has the best result as a matter of stability and less oscillation of magnitude and phase.

Figure 74. bode diagram to compare 3 controllers as green one is MPC, blue one is PID with derivative feedback and red one is auto-tuned PID in non-linear condition with sinusoidal input

In the same situation with sinus sweep input also is shown in figure 75:
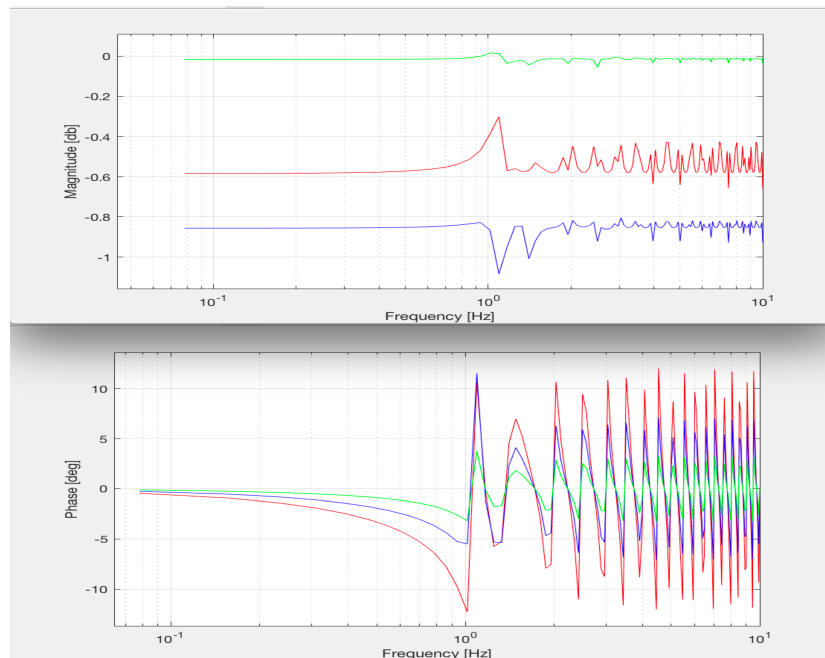

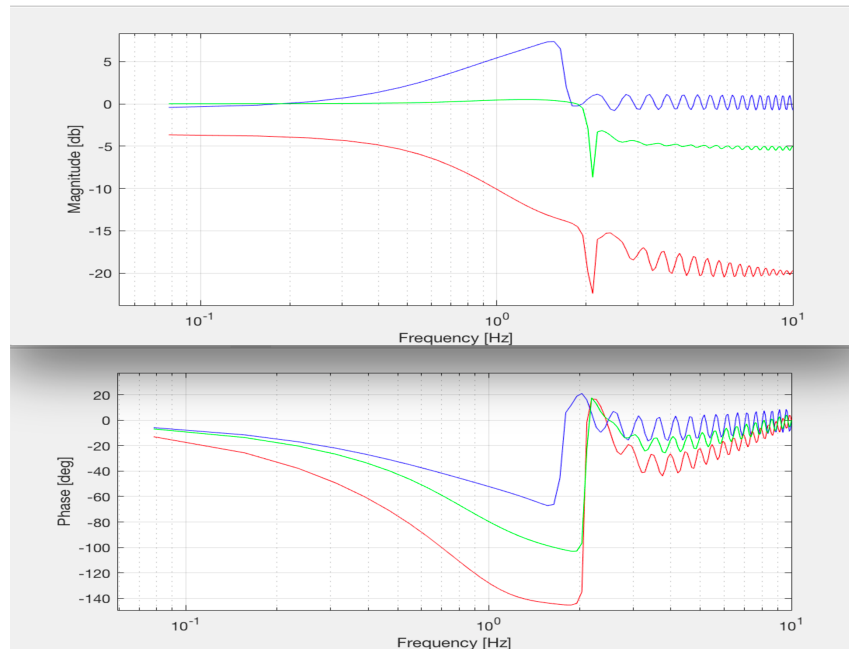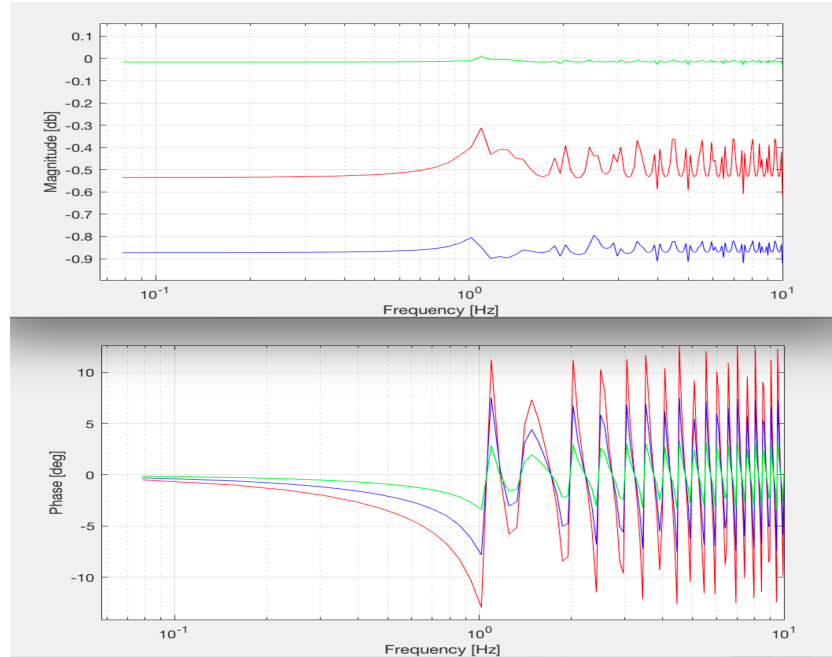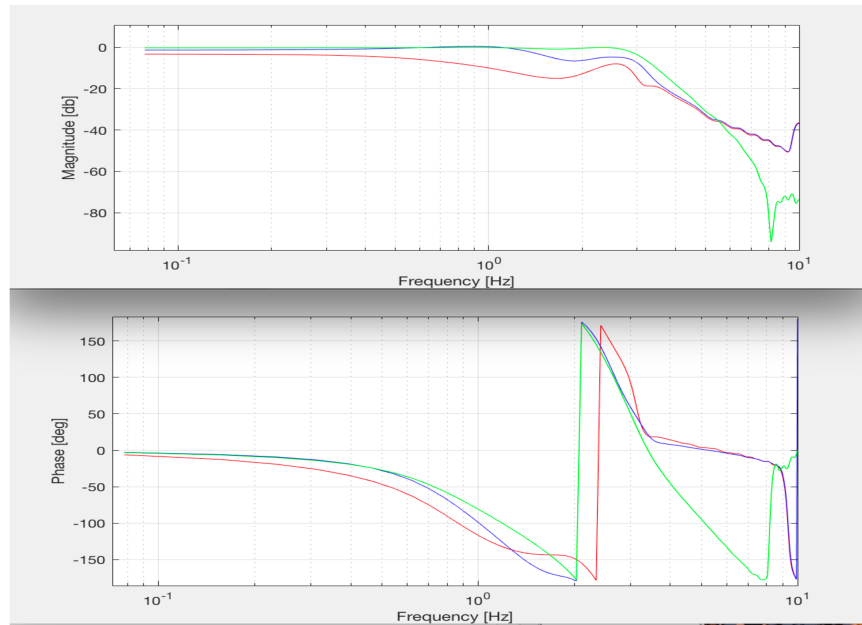Figure 75. bode diagram to compare 3 controllers as green one is MPC, blue one is PID with derivative feedback and red one is auto-tuned PID in non-linear condition with sinus-sweep input

In this situation, model controlled by MPC and PID with derivative feedback have almost very closed results but the auto-tuned PID does not have negligible difference in phase and magnitude in specific frequencies.

Now, to see the different results between linear and non-linear model environment behavior, each controller is tested separately as bellow.

Considering the auto-tuned PID first with sinusoidal input and then sinus sweep

Figure 76. bode diagram of the EPS system controlled by auto-toned PID with sinusoidal input by the red one is linear and blue is non-linear behavior

In figure 76 with sinusoidal input the phase shift is completely the same between linear and non-linear and the magnitude has slightly difference of 0.05 dB while, their trends are changed almost similar and the difference can be important when the precision of the model with respect to experimental one become critical. But in figure 77, sinus-sweep input condition has more realistic

71

results which the magnitude and phase are acting better in linear area than the non-linear one, which has around 150-degree difference in phase.

Figure 77. bode diagram of the EPS system controlled by auto-toned PID with sinus sweep input by the red one is linear and blue is non-linear behavior

For the system controlled by PID with derivative feedback, in figure 78 and 79, with sinus input there is about 0.3 dB difference in magnitude in 1.1 Hz and negligible deviation in phase. In sinus-sweep input again there is huge phase shift in specific frequency, like auto-tuned PID.

72

Figure 78. bode diagram of the EPS system controlled by PID with derivative feedback with sinusoidal input by the red one is linear and blue is non-linear behavior

Figure 79. bode diagram of the EPS system controlled by PID with derivative feedback with sinus-sweep input by the red one is linear and blue is non-linear behavior

73

The last controller is MPC which has also the same difference as other controllers between linear and non-linear area. In sinusoidal input condition has a bit difference only in magnitude and in sinus-sweep input situation has significant difference in phase about 150 degree.
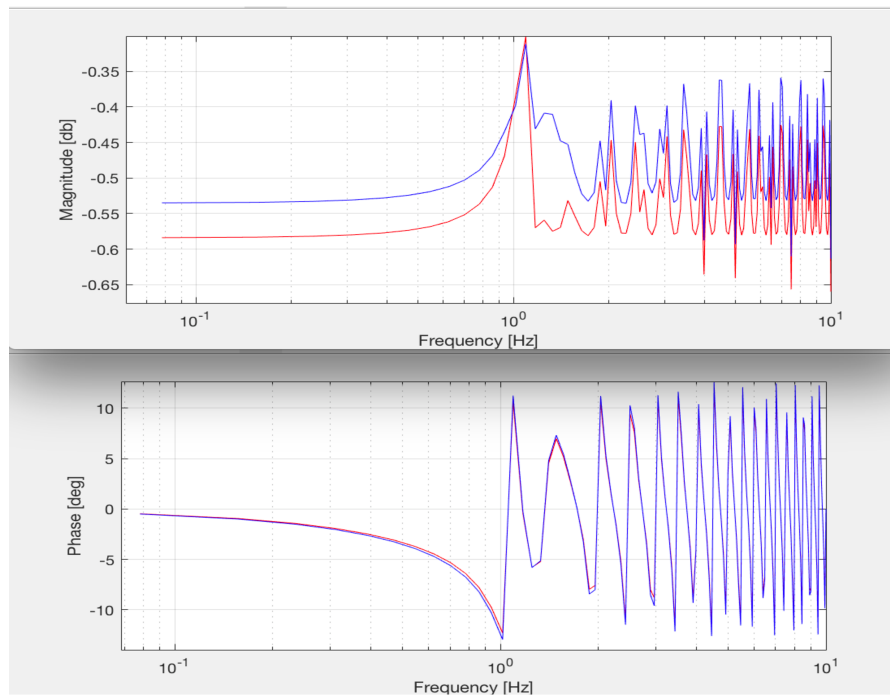

Figure 80. bode diagram of the EPS system controlled by MPC block with sinusoidal input by the red one is linear and blue is non-linear behavior
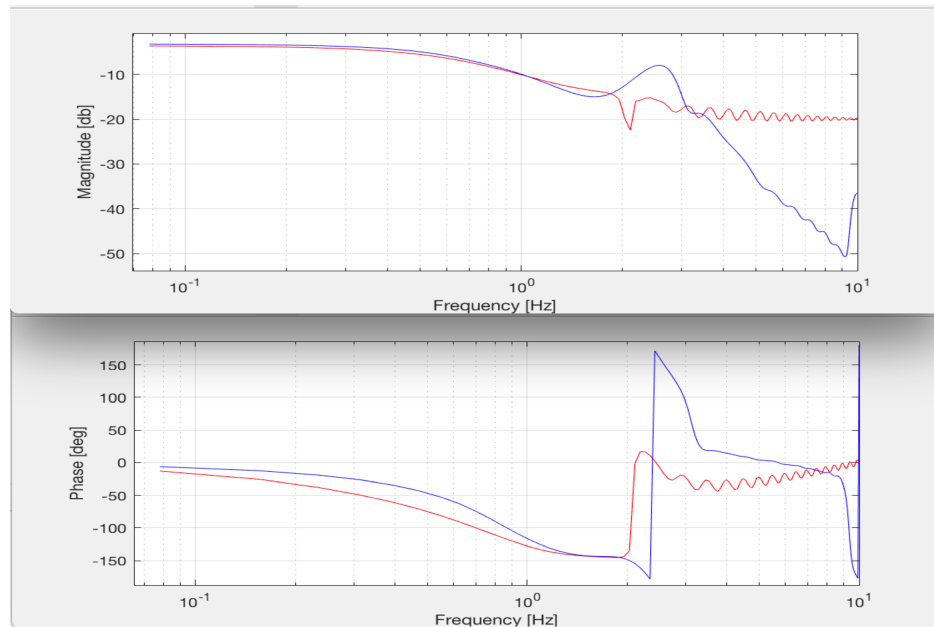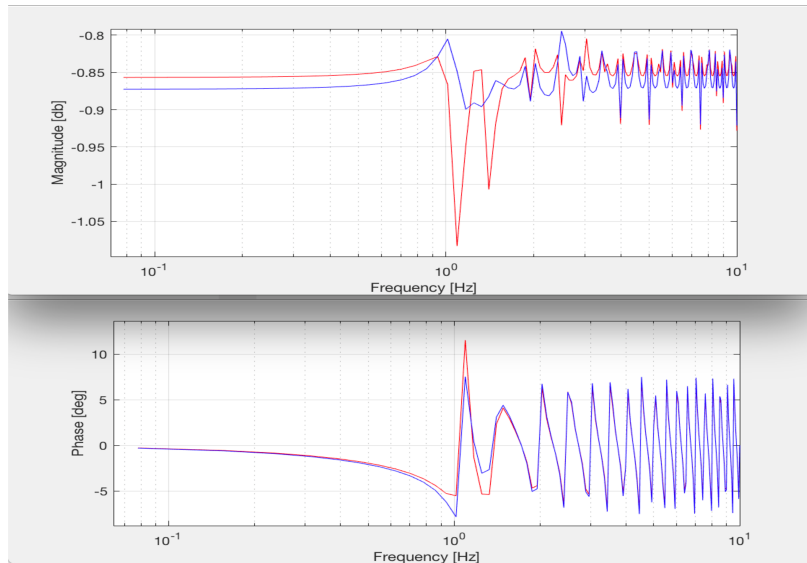

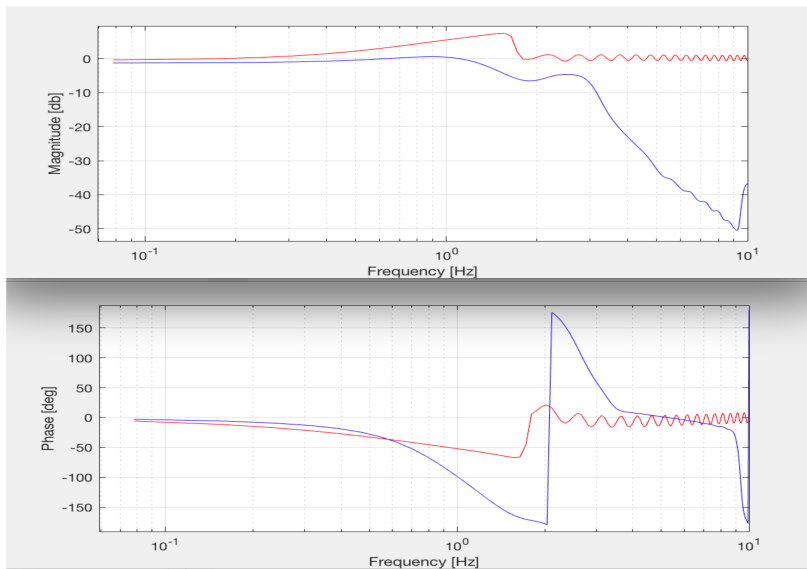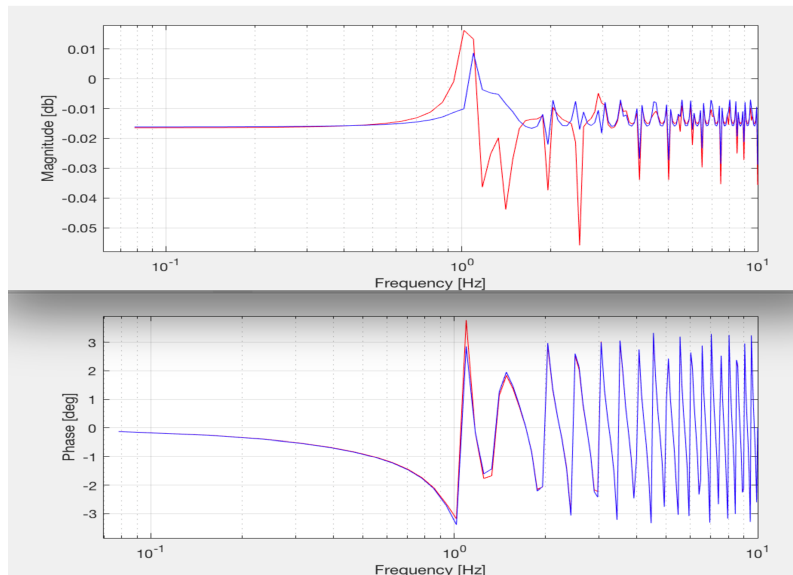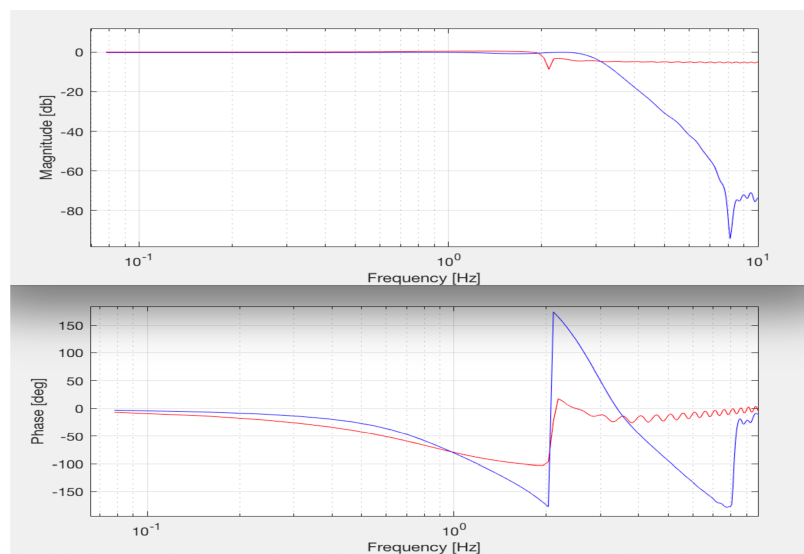Figure 81. bode diagram of the EPS system controlled by MPC block with sinus-sweep input by the red one is linear and blue is non-linear behavior

To conclude this part of comparison, the best controller in automotive functions is MPC block but a little unfriendly regulate in CarMaker area because of different working sampling time that is 0.01 in CarMaker and 0.1 in best MPC result. And linearization process in MPC block which cannot do the linearization process in CarMaker environment so it could be linearized in linear area then put it in nonlinear area with the same parameters. In any way, again has the best answers in non-linear IPG CarMaker model. As an alternative, the PID controller with derivative feedback can be used which we can also regulate and change the control coefficients in CarMaker.

About the difference between linear and non-linear area results, it can be said that with sinusoidal input by constant frequency the linear model also can be efficient with respect to the experimental hardware in loop test. But, in sinus sweep input when the frequency changed phase shift happened a lot.

With respect to the hardware in loop results, it can be compared with linear and non-linear result that leads to choose which model is more efficient to use in a complete vehicle system.

8. Conclusion

As the goal of this thesis, modeling the advance driver assistant system with considering the linear and non-linear friction in auto vehicles, to control the steering position in low speed driving, steering column part of the vehicle and three models of controller are designed for performing in a real-time simulation.

The steering column part was modeled based on Lagrange and bong graph approaches and implemented through matlab simulink block diagrams verified by real vehicle data provided by Fiat CRF. According to the vehicle natural frequency and the reference steering input torque, the model is excited in the frequency period of 0.7 to 2 Hz. So, This part singly has an acceptable frequency response while the ideal step input applied as the torque input the steering angle position start to change around 1.2Hz phase and amplitude.

The control strategies which are commonly used in automotive industry are PID and MPC controller. PID auto tunning block diagram , PID with derivative in feedback loop and the MPC block simulation are all had reasonable frequncy responses as expected and track the input motor torque trough the output of the EPS model to control the steering angle position. To test of this part, ideal stepinput at first and then the sinusoidal and chirp signal input were chosen for the input. To implement the designed model of the EPS and controller in the real-time simulation in IPG Carmaker the best controller was MPC compound with the EPS model inside the generic CarMaker model inside the vehicle control block which completely working in the maneuver of 10 Km/h speed and with sinusoidal, sinus sweep and IPG driver inputs tracking the output steering angle position. On the other hand, MPC block is hardly tunable in Carmaker area because of

different simulation order and sampling time but the best alternative can be PID controller with derivative feedback loop which has closed result to PMC.

So, the model almost has the acceptable answer in the real-time vehicle model provided by IPG Carmaker and it is ready for the future work to generate the code from the simulation and applied for the hardware in loop of the vehicle steering actuator.

References

1. Martina Joˇsevski, Alexander Katriniok,Andreas Riek Dirk Abel, Disturbance Estimation for Longitudinal Vehicle Dynamics Control at Low Speeds (2017), nternational Federation of Automatic Control Toulouse, France

2. Vivan Govender, Steffen Müller, Modelling and Position Control of an Electric Power Steering System (2016), published in Elsevier giornal.

3. Kandula, Prasanth Babu, "Dynamics and Control of an Electric Power Assist Steering System" (2010). Cleveland state university ETD archive.

4. J. Kim, J. Song, "Control Logic for an Electric Power Steering System Using Assist Motor," Mechatronics, vol. 12, no. 3, pp. 447-459, Apr. 2002.

5. X. Chen, T. Yang, X. Chen, K. Zhou, "A Generic Model Based Advanced Control of Electric Power Assisted Steering Systems," IEEE Transaction on Control Systems Technology, vol. 16, no. 6, Nov. 2008, pp. 1289-1300.

6. Shi Guobiao, Zhao Songhui, Min Jun, Simulation Analysis for Electric Power Steering Control System Based on Permanent Magnetism Synchronization Motor. (2012). International Conference (EMEIT).

7. Jeongjun Lee, Hyeongcheol Lee, Jihwan Kim, JiyoelJeong "Model-Based Fault Detection and Isolation for Electric Power Steering System", International Conference on Control, Automation and Systems, Oct. 17-20, 2007, COEX, Seoul, Korea

8. Gupta, Kumar, Purohit,   PID Control of Electric Power Steering System, published in research giornal of science and IT management.

9. Marcus Ljungberg, Electric power assist steering system parameterization and optimization employing CAE (2014), KTH university

10. L. and Hongqi, M. (2011), "EPS control based on state feedback", International Conference on Electric Information and Control Engineering (ICEICE), pp. 2154-7.

11. Aly Badawy, Jeff Zuraski, Farhad Bolourchi and Ashok Chandy, Modeling and Analysis of an Electric Power Steering System (1999), Delphi university

12. Shiang-Lung Koo, Fanping Bu, Han-Shue Tan, and Masayoshi Tomizuka, Vehicle Steering

Control under the Impact of Low-Speed Tire Characteristics, (2006) Proceedings of the American Control Conference Minneapolis, Minnesota, USA

13. Se-Wook OH, Ho-Chol CHAE, Seok-Chan YUN, Chang-Soo HAN, The design of controller for the steer-by-wire system, world Automotive congress

14. Jason Kong, Mark Pfeiffer, Georg Schildbach, Francesco Borrelli, Kinematic and Dynamic Vehicle Models for Autonomous Driving Control Design

15. Dariusz ardecki, MODELLING OF EPS TYPE STEERING SYSTEMS INCLUDING FREEPLAY AND FRICTION IN STEERING MECHANISM, journal of KONES Powertrain and Transport, Vol. 18, No. 1 (2011).

16. user manual Formula CarMaker$^{®}$ Tutorial 1.0, 1999 - 2016 by IPG Automotive GmbH – www.ipg.de

17. VU, T[rieu] M[inh], VEHICLE STEERING DYNAMIC CALCULATION AND SIMULATION, Annals of DAAAM for 2012 & Proceedings of the 23rd International DAAAM Symposium, Volume 23, No.1, ISSN 2304-1382 ISBN 978-3-901509-91-9, CDROM version, Ed. B. Katalinic, Published by DAAAM International, Vienna, Austria, EU, (2012)